ปริมาณรังสีและการประเมินความเสี่ยงจากรังสีของการตรวจเอกซเรย์คอมพิวเตอร์สมองในผู้ป่วยเด็ก

นางสาวศุภวรรณ จิวะพงศ์

วิทยานิพนธ์นี้เป็นส่วนหนึ่งของการศึกษาตามหลักสูตรปริญญาวิทยาศาสตรมหาบัณฑิต
สาขาวิชาฉายาเวชศาสตร์ ภาควิชารังสีวิทยา
คณะแพทยศาสตร์ จุฬาลงกรณ์มหาวิทยาลัย
ปีการศึกษา **2555**
ลิขสิทธิ์ของจุฬาลงกรณ์มหาวิทยาลัย

RADIATION DOSE AND RISK ESTIMATION IN PEDIATRIC

HEAD CT EXAMINATION

Miss Supawan Jivapong

A Thesis Submitted in Partial Fulfillment of the Requirements

for the Degree of Master of Science Program in Medical Imaging

Department of Radiology

Faculty of Medicine

Chulalongkorn University

Academic Year 2012

Thesis Title	RADIATION DOSE AND RISK ESTIMATION IN PEDIATRIC HEAD CT EXAMINATION
By	Miss Supawan Jivapong
Field of Study	Medical Imaging
Thesis Advisor	Associate Professor Anchali Krisanachinda, Ph.D.
Thesis Co-advisor	Assistant Professor Panruethai Trinavarat, M.D.
Thesis Co-advisor	Siri-on Tritrakarn, M.D.

Accepted by the Faculty of Medicine, Chulalongkorn University in Partial Fulfillment of the Requirements for the Master's Degree

…………………………….Dean of the Faculty of Medicine

(Associate Professor Sophon Napathorn, M.D.)

THESIS COMMITTEE

…………………………………..Chairman

(Associate Professor Sukalya Lerdlum, M.D.)

…………………………………..Thesis Advisor

(Associate Professor Anchali Krisanachinda, Ph.D.)

…………………………………..Thesis Co-advisor

(Assistant Professor Panruethai Trinavarat, M.D.)

…………………………………..Thesis Co-advisor

(Siri-on Tritrakarn, M.D.)

....External Examiner

(Professor Franco Milano, Ph.D.)

ศุภวรรณ จิวะพงศ์ : ปริมาณรังสีและการประเมินความเสี่ยงจากรังสีของการตรวจเอกซเรย์คอมพิวเตอร์สมองในผู้ป่วยเด็ก. (RADIATION DOSE AND RISK ESTIMATION IN PEDIATRIC HEAD CT EXAMINATION)

อ.ที่ปรึกษาวิทยานิพนธ์หลัก : รศ.ดร.อัญชลี กฤษณจินดา, อ.ที่ปรึกษาวิทยานิพนธ์ร่วม : ผศ. พญ. ปานฤทัย ตรีนวรัตน์ และ พญ. ศิริอร ตริตระการ 89 หน้า.

การตรวจด้วยเอกซเรย์คอมพิวเตอร์ในเด็กนั้น เป็นการแสดงภาพที่ดีเลิศ พบว่า มีอัตราการเพิ่มขึ้นประมาณ 10% ต่อปี มีผลให้ปริมาณรังสีที่ผู้ป่วยเด็กได้รับสูงเมื่อเทียบกับการตรวจวินิจฉัยทางรังสีด้วยวิธีอื่น เด็กมีความไวต่อผลของรังสี ที่ทำให้เกิดความเสียหาย และมีเวลานานในการสะสมรังสีตลอดชีวิต มากกว่าผู้ใหญ่ การศึกษานี้เป็นการศึกษาย้อนหลัง ในผู้ป่วยเด็กที่เข้ารับการตรวจเอกซเรย์คอมพิวเตอร์สมองที่โรงพยาบาลศิริราช ระหว่างเดือนกรกฎาคม - ธันวาคม 2554 จำนวน 145 ราย (79 เด็กชาย: 66 เด็กหญิง) ถูกแบ่งออกเป็น 4 กลุ่มอายุดังนี้ กลุ่มที่หนึ่งอายุ 0 ถึง 1 ปี 49 ราย (22:27), กลุ่มที่สอง มากกว่า 1 ถึง 5 ปี 40 ราย (27:13), กลุ่มที่สาม มากกว่า 5 ถึง 10 ปี 29 ราย (18:11) และกลุ่มที่สี่มากกว่า 10 ถึง 15 ปี 27 ราย (12:15) ปริมาณรังสียังผลคำนวนได้จากผลคูณค่า DLP กับค่าสัมประสิทธิ์การแปลง mSv.mGy-1.cm-1 สำหรับค่าปริมาณรังสีที่อวัยวะต่างๆ ได้แก่ สมอง, เลนส์ตา, ต่อมน้ำลาย, ผิวหนังและต่อมไทรอยด์ ปริมาณรังสีที่อวัยวะดูดกลืนถูกกำหนดโดยซอฟต์แวร์อิมแพคสแกนตาม ICRP 103 สำหรับการประเมินความเสี่ยงแบบสโตแคสติกใช้ค่าปริมาณรังสียังผลในการคำนวณ และใช้ค่าปริมาณรังสีที่อวัยวะในการประเมินความเสี่ยงแบบดีเทอร์มินิสติก

จากผลการศึกษาพบว่าค่าปริมาณรังสียังผล เท่ากับ 0.769, 0.7356, 0.7357 และ 0.764 มิลลิซีเวิร์ทในกลุ่มที่ 1-4 ตามลำดับ ค่าปริมาณรังสียังผลในแต่ละกลุ่มสอดคล้องกับความเสี่ยงจากรังสีรวมประมาณ 5.61 5.37, 5.37 และ 5.58 ต่อผู้ป่วย 100,000 ราย ที่เข้ารับการตรวจเอกซเรย์คอมพิวเตอร์สมอง ความเสี่ยงสูงสุดคือการเกิดมะเร็งเท่ากับ 3.85, 3.68, 3.68 และ 3.83 ต่อผู้ป่วย 100,000 ราย ความเสี่ยงต่ำสุดคือผลทางพันธุกรรมเป็น 10, 9.56, 9.56 และ 9.93 ต่อผู้ป่วย 1,000,000 รายที่เข้ารับการตรวจเอกซเรย์คอมพิวเตอร์สมอง ปริมาณรังสีที่อวัยวะในหน่วยมิลลิเกรย์ ของสมองกับต่อมน้ำลาย เลนส์ตา ผิวหนังและต่อมไทรอยด์ในกลุ่มที่ 1 เป็น 6.13, 6.36, 0.41 และ 0.19 มิลลิเกรย์, กลุ่มที่ 2 เท่ากับ 8.61, 9.85, 0.65 และ 0.47 มิลลิเกรย์, กลุ่มที่ 3 เท่ากับ 14.29, 15.06, 0.97, 0.75 มิลลิเกรย์และกลุ่มที่ 4 เท่ากับ 17.67, 18.67, 1.46 และ 0.99 มิลลิเกรย์ตามลำดับ การศึกษาครั้งนี้ทำการศึกษาปริมาณรังสีอวัยวะใน 1 ชุดมีค่าน้อยกว่า 0.02 เกรย์ ซึ่งต่ำกว่าค่าเกณฑ์ 0.5 เกรย์ ซึ่งจะก่อให้เกิดต้อกระจก ดังนั้น จะไม่เกิดผลดีเทอร์มินิสติก กับผู้ป่วยเด็กที่เข้ารับการตรวจเอกซเรย์คอมพิวเตอร์สมอง ที่ศูนย์ภาพวินิจฉัย โรงพยาบาลศิริราช สามารถสรุปได้ว่าผู้ป่วยเด็กที่เข้ารับการตรวจเอกซเรย์คอมพิวเตอร์สมอง ได้รับประโยชน์มากกว่าความเสี่ยงจากรังสี ค่าปริมาณรังสีในผู้ป่วยเด็กในการศึกษานี้เป็นแหล่งข้อมูลที่เป็นประโยชน์สำหรับผู้ปฏิบัติงานทางการแพทย์ เมื่อต้องอธิบายผลจากรังสีให้กับผู้ปกครองของผู้ป่วยเด็กบนพื้นฐานทางวิทยาศาสตร์ การศึกษาครั้งนี้ คาดหวังว่าจะได้รับความสนใจและให้ความสำคัญ กับความจริงที่ว่าเด็กไม่ใช่ 'ผู้ใหญ่ตัวเล็ก' และควรจะได้รับการปฏิบัติที่แตกต่างกัน

ภาควิชา :…....…รังสีวิทยา…….…....   ลายมือชื่อนิสิต…………………………………………

สาขาวิชา :…… ฉายาเวชศาสตร์……..   ลายมือชื่อ อ. ที่ปรึกษาวิยานิพนธ์หลัก…………………………

ปีการศึกษา :……...2555……….…....   ลายมือชื่อ อ. ที่ปรึกษาวิยานิพนธ์ร่วม…………………………

ลายมือชื่อ อ. ที่ปรึกษาวิยานิพนธ์ร่วม……………………………

##5474165930 :   MAJOR MEDICAL IMAGING
KEYWORDS : DOSE LENGTH PRODUCT (DLP), EFFECTIVE DOSE, ORGAN DOSE, PEDIATRIC CT HEAD, RADIATION PROTECTION

SUPAWAN JIVAPONG: RADIATION DOSE AND RISK ESTIMATION IN PEDIATRIC HEAD COMPUTED TOMOGRAPHY EXAMINATION. ADVISOR: ASSOC.PROF.ANCHALI KRISANACHINDA, Ph.D., 89 pp.

Pediatric CT study, an excellent imaging modality, has been increasing at about 10% per year. This has raised concerns because CT examinations deliver relatively high radiation dose compared to other X-ray diagnostic examinations. Children are much more sensitive to the damaging effects of ionizing radiation than adults and have a longer time to accumulate the radiation effect throughout their lives. This is a retrospective study in pediatric patients who underwent the CT brain at Siriraj Hospital between July and December 2011. 145 cases (79 boys: 66 girls) were divided into 4 age groups as follows: *Group1* 0-1 years 49 patients (22:27), *Group II* >1-5 years 40 cases (27:13), *Group III* >5-10 years 29 patients (18:11) and *Group IV* >10-15 years 27 patients (12:15). The effective dose has been determined from the multiplication of DLP and the conversion coefficient, $mSv.mGy^{-1}.cm^{-1}$ for head. The organ dose in brain, eye lens, salivary glands, skin and thyroid were determined by ImPACTSCAN software according to ICRP 103. Radiation risks have been estimated for stochastic effect from *effective dose* and deterministic effect from *organ dose.*

The results show the effective dose of group I – IV was 0.769, 0.7356, 0.7357 and 0.764 mSv respectively. The radiation risks as related to the effective dose were 5.61, 5.37, 5.37 and 5.58 per 100,000 pediatric patients undergoing head CT examination. Highest risk in cancer is 3.85, 3.68, 3.68 and 3.82 per 100,000 pediatric patients undergoing head CT examination. Lowest risk in hereditary effect was 10, 9.56, 9.56 and 9.93 per 1,000,000 individuals undergoing head CT examination. Organ doses in the brain/salivary gland, eye lens, skin and thyroid in group I were 6.13, 6.36, 0.41 and 0.19, group II 8.61, 9.85, 0.65, 0.47, group III 14.29, 15.06, 0.97, 0.75 and group IV 17.67, 18.67, 1.46 and 0.99 respectively. In this study each organ dose in one series is less than 0.02 Gy, resulted that the risk from cataract was not possible as the occurrence of cataract threshold is 0.5 Gy. Therefore, the deterministic effects would not occur for pediatric patient undergoing head CT examination at Imaging Center, Siriraj Hospital. It could be concluded that pediatric patients undergoing head CT examinations should have a benefit exceeds the small radiation risk. The radiation dose values in pediatric in this study is a useful source of information for medical workers when explaining the effects of radiation to parents of pediatric patients on scientific basis. This study looks forward to concerns and draws attention to the fact that children are not 'small adults', should be practiced differently.

Department………Radiology……..…	Student's Signature……………………....
Field of Study….Medical Imaging….	Advisor's Signature…………………………
Academic Year……...2012………….	Co-advisor's Signature………………...……
	Co-advisor's Signature………………...……

ACKNOWLEDGEMENTS

CONTENTS

LIST OF TABLES

Table **Page**

LIST OF FIGURES

LIST OF ABBREVIATIONS

Abbreviation	Terms
AAPM	American Association of Physicists in Medicine
ACR	American College of Radiology
cm	Centimeter
$CTDI_{vol}$	Volumetric computed tomography dose index
$CTDI_w$	Weighted computed tomography dose index
DLP	Dose-Length Product
DRLs	Diagnostic (dose) reference levels
E	Effective dose
FDA	Food and Drug Administration
Gy	Gray
ICRP	International commission on radiological protection
kVp	Kilo voltage peak
mm	Millimeter
mA	Milliampere
mAs	Milliampere-second
mGy	Milligray
mGy.cm	Milligray-centimeter
mSv	Millisevievert
MDCT	Multi-detector computed tomography
NRPB	National radiological protection board
PACS	Picture archiving and communication system
PMMA	Polymethymethacrylate

CHAPTER I

INTRODUCTION

1.1 Background and rationale

The number of CT examinations performed in the United States has been doubled for the past 5 years, with reports of more than 60 million performed yearly. 4–7 million of these examinations are performed in children [1]. Pediatric CT is an excellent imaging tool which has been increasing at a rate of about 10% per year recently. Increasing clinical use of pediatric CT has raised concerns because CT examinations deliver relatively high exposure doses compared with other X-ray diagnostic examinations.

In diagnostic radiology, the dose levels do not cause cell death and not enough to loss of organ function. Atom and molecules of cells will later be repaired, but repaired cells may vary from the original. A cell changes in somatic cells may be proliferation and induced cancer. Damage of gonad cells may have a genetic change and occur in the next generation.

This research involves the patients from neonate to young adult which the health care system is different. The pediatric patients are divided by age group of 0-1, >1-5, >5-10 and >10-15 years old. There is a special interest in children as the disease is specific with higher risk. Children are sensitive to the damaging effects of ionizing radiation than adults as explained in the table 1.1 because the children are not 'small adults' and should be observed differently.

Table 1.1 Reason and explanation for children concerned about risk of radiation than adults. [2]

Reason	Explanation
1. Higher biological sensitivity at same dose as adult	• More proliferating tissue • Different tissue distribution
2. Longer life expectancy	• Late manifestation of radiation induced cancer
3. Increase in dose and effective dose due to technical factors in radiological equipment	• Equipment often poorly adapted to pediatrics • Smaller size and close proximity of organs in children

As the U.S. patients have a right to know the dose from diagnostic radiation examination, the hospital must reduce the risk of being sued when patient dose exceeds a specified level (Dose Reference Level) without sufficient reasons. This may result in both acute and late effect, such as a skin injury and cancer. Therefore, the CT users must be aware of the risks from radiation. This project proposes the methods to reduce the risks that may occur in the future with the increasing use of CT, especially in pediatric patients.

The main objective of this research is to emphasize the radiation safety of patients who underwent head computerized tomography examination at Siriraj Hospital.

U.S. FOOD AND DRUG ADMINISTRATION Report: Safety Investigation of CT Brain Perfusion Scans: Initial Notification Date Issued: October 8, 2009 [3]

Over an 18-month period, 206 patients at a particular facility received radiation doses from CT brain perfusion that were approximately eight times the expected level. Instead of receiving the expected dose of 0.5 Gy (maximum) to the head, these patients received 3-4 Gy. As a result of using protocol which amount of radiation is higher than expected. Although the machine was used for different scans, all patients who received a CT brain perfusion were the only patients affected. In some cases, this excessive dose resulted in hair loss and erythema.

Although the balance between risks and benefits remains strongly tilted toward benefit, there is still need for caution. In addition, the frequency of pediatric CT examinations is increased rapidly, and estimate that quantitative lifetime radiation risks for children is not trivial. Therefore, the radiation dose and risk estimation in pediatric head CT examination must be studied.

1.2 Objective

To evaluate the radiation dose with its affecting factors and risk estimation in pediatric head CT examination.

CHAPTER II

REVIEW OF RELATED LITERATURES

2.1 Theory

2.1.1 The introduction of CT

Computed tomography (CT) is a medical imaging procedure used to create a tomography image of the body. They provide anatomical information by the principle that different types of tissues, their composition and density, absorb varying amount of x-rays. CT produces a volume of data that can be manipulated, through "windowing", to demonstrate various physical structures. Although historically the images generated were in the axial or transverse plane, orthogonal to the long axis of the body, modern scanners allow this volume of data to be reformatted in various planes or even as volumetric (3D) representations of structures [4].

The basic components of CT scanner are a gantry, a patient couch, hardware equipment, an operator console and workstations. The gantry is a doughnut - shaped ring containing the x-ray tube, the detector array and associated equipment. The central hole in the gantry accommodates the patient on a sliding table (Figure 2.1). The x-ray tube rotates around a slice of patient anatomy. This slice represents the X - Y plane, with the X - axis being horizontal and the Y - axis vertical. The isocenter of the gantry is the central point of this plane. The third dimension is represented by the Z - axis, which is along the orientation of the patient couch. A motorized table moves the patient through the CT imaging system. At the same time, a source of x-rays rotates within the circular opening, and a set of x-ray detectors rotates in synchrony on the far side of the patient.
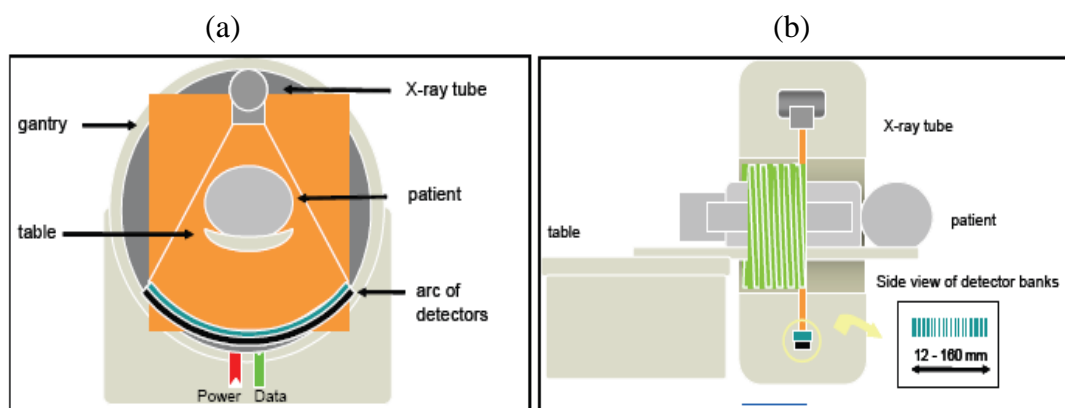
Figure 2.1 Diagram of CT scanner (a) 'End view', (b) 'Side view' in helical acquisition mode

MDCT systems are CT scanners with a detector array consisting of more than a single row of detectors. The "multi-detector-row" nature of MDCT scanners refers to the use of multiple detector arrays (rows) in the longitudinal direction. MDCT scanners utilize third generation CT geometry in which the arc of detectors and the x-ray tube rotate together. All MDCT scanners use a slip-ring gantry, allowing helical acquisition at rotation speeds as fast as 0.33 second for a full rotation of 360 degrees of the X-ray tube around the patient. A scanner with two rows of detectors had already been on the market since 1992 and MDCT scanners with four detector rows were introduced in 1998 by several manufacturers [5]. The primary advantage of these scanners is the ability to scan more than one slice simultaneously and hence more efficiently use the radiation delivered from the X-ray tube. The time required to scan a certain volume could thus be reduced considerably.

MDCT scanners can cover a specific anatomic volume with thinner slices. This considerably improves the spatial resolution in the longitudinal direction without the drawback of extended scan times. Improved resolution in the longitudinal direction is of great value in multiplanar reformatting (MPR, perpendicular or oblique to the transaxial plane) and in 3-dimensional (3D) representations. Spiral scanning is the most common scan acquisition mode in MDCT, since the total scan time can be reduced most efficiently by continuous data acquisition and overlapping data sets and this allows improved multi-planar reconstruction (MPR) and 3D image quality to be reconstructed without additional radiation dose to the patient.

One of the most important applications of CT is in head trauma, where it is used to investigate possible skull fractures, underlying brain damage, or hemorrhage. Hemorrhage shows up on CT scans as areas of increased intensity due to higher attenuation from the high levels of protein in hemoglobin. Edema often associated with stroke, shows up as an area of reduced intensity on the image. For brain tumors, CT is excellent at showing calcification in lesions such as meningiomas or gliomas, and can be used to investigate changes in bone structure and volume in diseases of the sinus. In well-vascularized tumors such as meningiomas, iodinated contrast agents are often injected, and increase the intensity of the tumor. In healthy brain tissue, the blood brain barrier (BBB) selectively filters the blood supply to the brain, allowing only a limited number of naturally occurring substrates to enter brain tissue. If the brain is damaged, by a tumor, for example, the BBB is disrupted such that the injected contrast agent can now enter the brain tissue. As tumors grow, they develop their own blood supply, and blood flow is often higher in tumors, particularly in the periphery of the tumor, than in normal tissue. Abscesses, for example, often show a distinctive pattern in which the center of the pathology appears with a lower signal than surrounding tissue, but is encircled by an area of higher signal, a so-called "rim enhancement".

2.1.2 Factors affecting the radiation dose in CT examination

The scanning parameters selected to obtain the minimum radiation dose during examinations are kVp, mA, scan time, slice collimation, slice thickness and pitch. Setting kVp and mA depends on age and body thickness. Increasing scan speed by shorter rotation time and a wider beam will cover the entire scan volume, thus, the incidence of motion artifacts is reduced. This will be benefit in the reduction of the repeat examinations. The use of narrow collimation decreased geometric efficiency with CT scanners and lead to an increase in dose exponentially, decreases partial volume averaging and hence improves contrast for small objects. Consequently, images with higher noise levels would reduce diagnostic accuracy, the contrast to noise ratio may be similar or improved. Pitch should be balanced with patient dose and image quality. Pitch higher than 1.0 can reduce motion artifact and decrease radiation dose. The radiation doses to particular organs from any given CT study depend on the number of scans, mAs, the size of the patient, the axial scan range, the scan pitch (the degree of overlap between adjacent CT slices), the tube voltage in the kilovolt peaks (kVp), and the specific design of the scanner being used. The relative noise in CT images increase as the radiation dose decreases, which means that there will always be a tradeoff between the need for low-noise images and the desirability of using low doses of radiation **[6]**.

2.1.3 CT radiation dose

The radiation dose from CT examination is defined as the weighted CT Dose Index, $CTDI_w$ and the CT Dose Index for irradiated volume of tissue, $CTDI_{vol}$ with the unit of mGy, and the dose length product, DLP with the unit of mGy.cm.

2.1.3.1 Computed tomography dose index (CTDI).

The CTDI is the primary dose measurement concept in CT,

$$CTDI = \frac{1}{nT} \int_{-\infty}^{\infty} D(z)dz$$

Where n is the number of slices acquired

T is the nominal slice thickness

$D(z)$ is the radiation dose measured at position z along the scanner's axis.

CTDI represents the average absorbed dose, along the z-axis, from a series of contiguous irradiations. It is measured from one axial CT scan (one rotation of the x-ray tube), and is calculated by dividing the integrated absorbed dose by the nominal total beam collimation. Reference dosimetry for CT is based on such measurements made within standard CT dosimetry phantoms; these presently comprise homogeneous cylinders of polymethylmethacrylate (PMMA), with diameters of 16 cm (head) and 32 cm (body), although phantoms of water-equivalent plastic and with elliptical cross-sections are under development. Typically, the dose distribution within the body cross section imparted by a CT scan is much more homogeneous than that imparted by radiography, but is still somewhat larger near the skin than in the body center. Therefore, the combination of measurements made at the centre (c) and 10 mm below the surface (p) of a phantom leads to weighted CTDI in the standard head or body phantom for a single rotation corresponding to the exposure settings used in clinical practice:

$$\text{CTDI}_w \; = \; \frac{1}{3}\,\text{CTDI}_{100,c} \; + \; \frac{2}{3}\,\text{CTDI}_{100,p}$$

where CTDI_{100},p represents an average of measurements at four different locations around the periphery of the phantom.

2.1.3.2 Dose-length product

To better represent the overall energy delivered by a given scan protocol, the absorbed dose can be integrated along the scan length to compute the Dose-Length Product where:

$$\text{DLP (mGy-cm)} \; = \; \text{CTDI}_{vol} \text{ (mGy) x scan length (cm)}$$

The DLP reflects the total energy absorbed attributable to the complete scan acquisition. Thus, an abdomen-only CT exam might have the same CTDI_{vol} as an abdomen/pelvis CT exam, but the latter exam would have a greater DLP, proportional to the greater z-extent of the scan volume.

The CTDI_{vol} and the DLP values are displayed on the scanner console. It is always invaluable to look at these figures when reviewing patient images for an assessment of the image quality and dose performance of a scanner. Both the CTDI_{vol} and the DLP are used when comparing with dose reference levels (DRLs). MDCT scanners have the potential to give higher radiation doses compared to single slice scanners. Their flexibility in scanning long lengths with high mAs values, and the ease with which they perform dual and even triple-phase contrast studies, can lead to high patient doses. In addition, there are some intrinsic features of current MDCT design which can give rise to slightly higher doses.

2.1.3.3 Effective dose

The effective dose is a "dose" parameter that reflects the risk of a non-uniform exposure in terms of a whole body exposure. It is a concept used to normalize partial body irradiations relative to whole body irradiations to enable comparisons of risk (International Commission on Radiological Protection, 1991). Effective dose is expressed in the units of milliSieverts (mSv). The calculation of effective dose requires knowledge of the dose to specific sensitive organs within the body, which are typically obtained from Monte Carlo modeling of absorbed organ doses within mathematical anthropomorphic phantoms, and recently also voxel phantoms based on real humans.

Effective dose values calculated from the NRPB Monte Carlo organ coefficients [6] were compared to DLP values for the corresponding clinical exams to determine a set of coefficients *k*, where the values of *k* are dependent only on the region of the body being scanned (Table 2.1). Using this methodology, *E* can be estimated from the DLP, which is reported on most CT systems:

$$E \text{ (mSv)} = k \; \text{ x } \; \text{DLP}$$

where k is a weighting factor (mSv $\times$ mGy^{-1} $\times$ cm^{-1}) depends only upon body regions

Table 2.1 Normalized effective dose per dose-length product (DLP) for pediatric patients of various ages [7].

Age	k (mSv $\bullet$ mGy^{-1} $\bullet$ cm^{-1})*
0 year	0.0110
1 year	0.0067
5 year	0.0040
10 year	0.0032

*Conversion factor for pediatric patients assumes use of the head phantom (16 cm).

The values of E predicted by DLP and the values of E estimated using more rigorous calculations methods are remarkably consistent. Hence, the use of DLP to estimate E appears to be a reasonably robust method for estimating effective dose.

2.1.3.4 Organ dose

Organ dose is the absorbed dose in matter and tissue resulting from the exposure to indirect and direct ionizing radiation. The organ dose (or the distribution of dose in the organ) will largely determine the level of risk to that organ from the radiation. Organ dose is measured in grays (Gy). One gray equals 1 joule of radiation energy absorbed per kilogram. It can calculate or estimate many methods such as Monte Carlo model, software tool available, and the gold standard method is measurement with TLD in anthropomorphic phantoms.

2.1.4 DRLs

Diagnostic reference levels (DRLs) were first mentioned by the International Commission on Radiological Protection (ICRP) in 1990 **[8]** and subsequently recommended in greater detail in 1996. DRLs are not the suggested or ideal dose for a particular procedure or an absolute upper limit for dose. Rather, they represent the dose level at which an investigation of the appropriateness of the dose should be initiated. In conjunction with an image quality assessment, a qualified medical physicist should work with the radiologist and technologist to determine whether or not the required level of image quality could be attained at lower dose levels. Thus, reference levels act as "trigger levels" to initiate quality improvement.

The Commission now recommends the use of diagnostic reference levels for patients. These levels, which are a form of investigation level, apply to an easily measured quantity, usually the absorbed dose in air, or in a tissue equivalent material at the surface of a simple standard phantom or representative patient. The diagnostic reference level will be intended for use as a simple test for identifying situations where the level of patient dose or administered activity is unusually high. If it is found that procedures are consistently causing the relevant diagnostic reference level to be exceeded, there should be a local review of procedures and the equipment in order to determine whether the protection has been adequately optimized. If not, measures aimed at reduction of doses should be taken. Diagnostic reference levels are supplements to professional judgment and do not provide a dividing line between

good and bad medicine. It is inappropriate to use them for regulatory or commercial purposes. Diagnostic reference levels apply to medical exposure, not to occupational and public exposure. Thus, they have no link to dose limits or constraints. Ideally, they should be the result of a generic optimization of protection. The values should be selected by professional medical bodies and reviewed at intervals that represent a compromise between the necessary stability and the long-term changes in the observed dose distributions. The selected values will be specific to a country or region.

In Table 2.2, examples of UK national reference doses for head trauma (including non accidental injury) pediatric patients from various age groups. The $CTDI_w$ values are provided for the purpose of comparison with historical values as this index has largely been replaced by $CTDI_{vol}$ as a reference dose quantity. For examinations on children, $CTDI_{vol}$ and DLP decrease with decreasing age.

Table 2.2: UK National Reference Doses for Head Trauma CT on Pediatric Patients (including non accidental injury), published 2006 following 2003 review, compared with EU values from 2000 [9]

Ages	Region	$CTDI_w$ (mGy)		$CTDI_{vol}$ (mGy)	DLP (mGy cm)	
		UK 2003	Europe	UK 2003	UK 2003	Europe
	Post Fossa	35	-	35	-	-
0-1 year	Cerebrum	30	-	30	-	-
	Whole exam	--	40	-	270	300
	Post Fossa	50	-	50	-	-
5 year old	Cerebrum	45	-	45	-	-
	Whole exam	--	60	--	470	600
	Post Fossa	65	-	65	-	-
10 year 0ld	Cerebrum	50	-	50	-	-
	Whole exam	--	70	--	620	750

2.1.5 Biological effects

The effects of ionizing radiation in human can be divided into two categories.

1. Deterministic effect occurs after large exposures. The severity depends upon the radiation dose. The higher dose leads to the greater effect. There is a threshold for deterministic effects. The examples of this effect are the skin injury, cataract and hair loss.

2. Stochastic effect appears after a long latent period. This effect has no radiation threshold. Stochastic effects occur randomly and depend on the type of ionizing radiation administered, the tissue receiving the radiation, and the age of the subject. The severity of the result is the same but the probability of occurrence increases with radiation dose. The examples of this effect are cancer and hereditary effects.

Deterministic effect estimation in each organ depends on absorbed dose and tissue weighting factor. Critical organs with high radiosensitivity in head CT are eye lens and thyroid. While the radiation dose from the head CT examination may not be high enough to produce deterministic effect but stochastic effect should be considered.

2.1.6 Pediatric CT

The growth of CT use in children has been driven primarily by the decrease in the time needed to perform a scan, largely eliminating the need for anesthesia to prevent the child from moving during image acquisition. Children are more susceptible to risk of radiation induced carcinogenesis compared to adults. Therefore, radiologists, medical physicists, and technologists, must pay special attention to CT scan protocols and radiation dose when imaging children.

Physicians can use the CT examination to help detect a wide range of abnormalities, including those from injury or illness, in almost any part of a child's body. In children, CT is typically used to diagnose causes of abdominal pain, evaluate for injury after trauma, diagnose and stage cancer, monitor response to treatment for cancer, and diagnose and monitor infectious or inflammatory disorders. CT may also be performed to evaluate blood vessels throughout the body. With CT, it is possible to obtain very detailed pictures of the heart and large blood vessels in children, even newborn infants.

There is always a slight chance of cancer from excessive radiation exposure. However, the benefit of an accurate diagnosis far outweighs the risk. Radiation is necessary to obtain CT images. It is known that high levels of radiation may cause cancer. However, CT scans result in a low-level exposure [10]. Whether such levels cause cancer is debatable but because it is possible, every effort is made to limit the amount of radiation children may receive from a CT scan. One of the best ways of limiting radiation exposure is to avoid CT scans that are not clearly needed. Another strategy is to consider other tests, such as MRI or ultrasound which might give the same information. Because children are more sensitive to radiation, they should have a CT study only if it is essential for making a diagnosis and should not have repeated CT studies unless absolutely necessary.

2.1.7　Radiation protection in pediatric CT

The important issues on radiation protection are not only the frequencies of radiological examinations but also how to perform justification and optimization considering with both risks and benefits. In addition to that, the protection for pediatric patients is also important because of their radiation sensitivities. While the situation in pediatric CT is not fully documented, the above has led to increasing concern about the exposure of children, particularly as adult scan settings were for many years used in pediatric CT.

2.1.7.1 Justification in pediatric CT

This is not surprising as some reports have estimated that between a third and half of the examinations occurring may not be necessary, and many are conducted using inappropriate technical factors **[11]**. Attention should be paid to age-specific pathology, its prognosis, individual pediatric questions, the costs and the radiation exposure involved in an examination. Previous examinations must be considered, as implied by the proposed IMAGE GENTLY/IAEA record card. This may render the procedure under consideration unnecessary or allow it be replaced by a less dose intensive one. Likewise, the potential contribution of the scan to the management and outcome of the patients' condition should be considered. Follow-up examinations should be delayed unless therapeutic decisions based on them are needed immediately.

2.1.7.2 Optimization in pediatric CT

Many aspects of the acquisition of a study affect radiation dose and image quality. These must be optimized. Optimization is facilitated if the patient is well prepared so that the examination can proceed smoothly. Check or confirm renal function and verify hydration where relevant. Place intravenous lines well in advance. Take whatever steps are desirable to decrease anxiety and movement, including avoiding pain and, where valuable, the use of medication, sedation, anesthetics, immobilization and positioning aids etc. Appropriate information must be provided to both the patient and accompanying persons.

2.1.8 Typical organ doses

Organ doses from CT scanning are considerably larger than those from corresponding conventional radiography. The number of scans in a given study is, of course, an important factor in determining the dose. The radiation doses to particular organs from any given CT study depend on a number of factors. The most important are the number of scans, the tube current and rotation time in milliamp-seconds (mAs), the size of the patient, the axial scan range, the scan pitch (the degree of overlap between adjacent CT slices), the tube voltage in the kilovolt peaks (kVp), and the specific design of the scanner being used.

Many of these factors are under the control of the radiologist or radiographer. Ideally, they should be tailored to the type of study being performed and to the size of the particular patient, a practice that is increasing but is by no means universal. It is always the case that the relative noise or graininess in CT images will increase as the radiation dose decreases, which means that there will always be a tradeoff between the need for low-noise images and the desirability of using low doses of radiation. It is important that mAs is a major factor affecting contrast resolution as it directly influences the number of x-ray photons used to produce the CT image, thereby affecting the SNR and contrast resolution. Doubling the mAs, increases the SNR by or 41% and contrast resolution consequently improves **[12]**.

2.2 Review of Related Literature

Many researchers studied the radiation dose in pediatric computed tomography such as Kritsaneepaiboon1 S, Trinavarat P and Visrutaratna P **[13]** survey the radiation dose CT in children in three university hospitals in Thailand in four age groups using the CT dose index (CTDI) and dose length product (DLP). Performed retrospective review of CT dosimetry in pediatric patients who had undergone head, chest, and abdominal MDCT in three major university hospitals in Thailand. CTDIvol and DLP were recorded, categorized into four age groups: <1 year, $1 -\!\!<$ 5 years, $5 -\!\!<$ 10 years, and $10 -\!\!<$ 15 years. Results in per age group, the third quartile values for brain, chest, and abdominal CTs were, respectively, *in terms of CTDI$_{vol}$*: 25, 30, 40, and 45 mGy; 4.5, 5.7, 10, and 15.6 mGy; 8.5, 9, 14, and 17 mGy; and *in terms of DLP*: 400, 570, 610, and 800 mGy cm; 80, 140, 305, and 470 mGy cm; and 190, 275, 560,765 mGy.cm. This preliminary national dose survey for pediatric CT in Thailand found that the CTDI$_{vol}$ and DLP values in brain, chest, and abdominal CTs were still below the diagnostic reference levels from the UK and Switzerland recommendation.

Fujii K, et al. **[14]** studied the organ doses in infant CT examinations with MDCT scanners. Radiation doses were measured by radio-photoluminescence glass dosemeter sets in various organ positions within a 1-year-old child anthropomorphic phantom and organ doses were evaluated from the measurement values. Doses for tissues or organs within the scan range were 28–36 mGy in an infant head CT, 3–11 mGy in a chest CT, 5–11 mGy in an abdominal-pelvic CT and 2–14 mGy in a cardiac CT. The doses varied by the differences in the types of CT scanners and scan parameters used at each medical facility. Compared with those for children of various ages, the doses in an infant CT protocol were found to be similar to or slightly smaller than those in a pediatric CT for 5- or 6-year-old children. These results would show that scan parameters appropriate for infants were routinely used at each medical facility. This would also indicate the potential of further dose reduction by the adjustment of scan parameters on the basis of individual patient's weight. Dose data evaluated in this study would lead to the optimization of scan parameters and would also be useful for the estimation of radiation risks for infants in CT examinations.

Huda W. **[15]** studied the effective doses and the corresponding risks of radiation-induced cancers for patients undergoing chest CT examinations. Patient dose determination was based on the characteristics of 16-slice CT scanner from 4 vendors. The dose length product (DLP) was used to quantify the amount of radiation used to perform chest CT examinations. DLP was converted into a corresponding effective dose (E) using age-dependent E/DLP conversion coefficients applicable to chest CT examinations. Calculations of effective doses were performed for a typical chest CT examination, as well as for a low dose protocol for patients with cystic fibrosis. Effective doses were used to estimate nominal cancer risks based on data of the Committee of the Biological Effects of Ionizing Radiation (BEIR). Patient effective doses in standard chest CT examinations range from approximately 1.7 mSv in newborns to approximately 5.4 mSv in adults. The effective dose to a 5-year-old patient with cystic fibrosis using a low-dose protocol is approximately 0.55 mSv, corresponds to a nominal excess risk of carcinogenesis of approximately 1.5 cancers per 10,000 individuals, with half of these being fatal. It is concluded that patients undergoing chest CT examinations should have a benefit that exceeds the small radiation risk.

Huda W, et al. **[16]** determined the effective dose (E) per unit dose-length product (DLP) conversion factors for CT dosimetry. A CT dosimetry spreadsheet was used to compute patient E values and corresponding DLP values. The ratio of E to DLP was determined with 16-slice CT scanners from four vendors, as well as with five models from one manufacturer that spanned more than 25 years. E-to-DLP ratios were determined for 2-cm scan lengths along the patient axis, as well as for typical scan lengths encountered at head and body CT examinations. The dependence of the ratio of E to DLP on x-ray tube voltage (in kilovolts) was investigated, and the values obtained with the spreadsheet were compared with those obtained by using two other commercially available CT dosimetry software packages. For 2-cm scan lengths, changes in the scan region resulted in differences to E, but much lower variation was obtained for typical scan lengths at clinical head and body imaging. Inter- and intra manufacturer differences for E/DLP were generally small. Representative values of E/DLP at 120 kV were 2.2 μSv/mGy.cm (head scans), 5.4 μSv/mGy.cm (cervical spine scans), and 18 μSv/mGy.cm (body scans). For head scans, E/DLP was approximately independent of x-ray tube voltage, but for body scans, the increase from 80 to 140 kV increased the ratio of E to DLP by approximately 25%.

Mazonakis M, et al. **[17]** estimated thyroid dose and the associated risk for thyroid cancer induction from common head and neck CT examinations during childhood. The Monte Carlo N-particle transport code was employed to simulate the routine CT scanning of the brain, paranasal sinuses, inner ear and neck performed on sequential and/or spiral modes. The mean thyroid dose was calculated using mathematical phantoms representing a newborn infant and children of 1, 5, 10 and 15 years old. To verify Monte Carlo results, dose measurements were carried out on physical anthropomorphic phantoms using thermoluminescent dosemeters (TLDs). The scattered dose to thyroid from head CT examinations varied from 0.6 to 8.7 mGy depending upon the scanned region, the pediatric patient's age and the acquisition mode. Primary irradiation of the thyroid gland during CT of the neck resulted in an absorbed dose range of 15.2–52.0 mGy. The mean difference between Monte Carlo calculations and TLD measurements was 11.8%. Thyroid exposure to scattered radiation from head CT scanning is associated with a low but not negligible risk of cancer induction of 4–65 per million patients. Neck CT can result in an increased risk for development of thyroid malignancies up to 390 per million patients.

Xiang Li, et al **[18]** estimated the patient-specific radiation dose and cancer risk for pediatric chest CT examination and evaluated factors affecting dose and risk, including patient size, age, and scanning parameters. This study included 30 patients between 0 to16 years old. A validated Monte Carlo program was used to estimate organ dose from eight chest protocols, representing clinically relevant combinations of bowtie filter, collimation, pitch, and tube potential. Organ dose was used to calculate effective dose and risk index (an index of total cancer incidence risk). Organ dose normalized by tube current–time product (mAs) or $CTDI_{vol}$ decreased exponentially with increasing average chest diameter. Effective dose normalized by tube current–time product or DLP decreased exponentially with increasing chest diameter. Chest diameter was a stronger predictor of dose than weight and total scan length. Risk index normalized by tube current–time product or DLP decreased exponentially with both chest diameter and age. The correlations of dose and risk with patient size and age can be used to estimate patient-specific dose and risk.

CHAPTER III

RESEARCH METHODOLOGY

3.1 Research Design

This study is an observational descriptive research.

3.2 Research Design Model
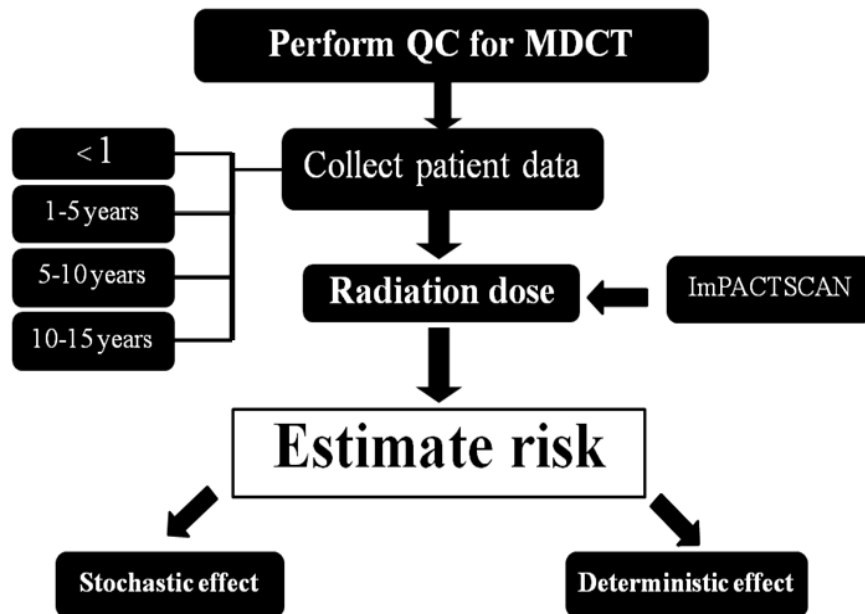
3.3 Conceptual framework
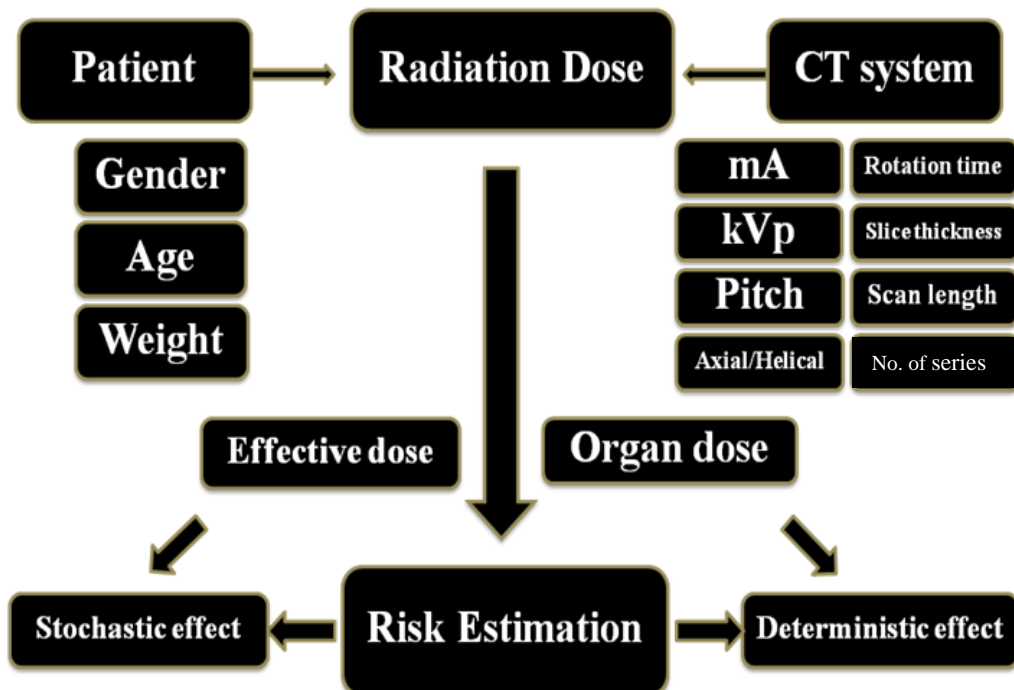
3.4 Key words

- Dose Length Product (DLP)
- Effective dose
- Organ dose
- Pediatric CT head

3.5 Research question

1. What are the radiation dose and factors affecting in pediatric head CT examination?

2. What are the radiation risks in pediatric head CT examination?

3.6 Materials

3.6.1 CT scanner: 64 slices CT, manufacturer GE model LightSpeed VCT (Figure 3.1), installed at Faculty of Medicine Siriraj Hospital in the year 2005.

Figure 3.1 64 slices CT, manufacturer GE model LightSpeed VCT

64 slices CT GE LightSpeed VCT, computer software unit with the operating system Linux and the application software Advantage Workstation 4.2 model 07MW18.4 for acquisition and processing, at Imaging Center, Department of Radiology, Faculty of Medicine Siriraj Hospital, had been used in this study. CT scanner was installed in 2005. The GE LightSpeed VCT is the third-generation multi-detector CT scanner, featuring a 100 kW generator, 140 kVp maximum, 715 mA maximum and fastest gantry rotation time of 0.35 seconds. It is capable of imaging 64 slices per rotation, with slice widths of 64 x 0.625 mm only cardiac protocol and 16 x 1.25 for other protocols.

3.6.2 PMMA Phantom

The CT phantoms had been used to perform QC for CT system. The phantoms are manufactured to comply with the FDA's performance standard for diagnostic x-ray systems. Two cylindrical phantoms were made of solid Polymethyl Methacrylate (PMMA) of 16 cm (head), 32 cm (body) in diameter and 14 cm length.

There are 5 holes with acrylic rods to plug in the holes for both phantoms when not use for exposure. Through holes are 1.31 cm in diameter and 14 cm length to accommodate standard CT probes. One is at center and four are around the perimeter, 90º apart and 1 cm hole center to the outside edge of each phantom.

3.6.3 Catphan ® 600 phantom

Catphan ® 600 phantom will be used for the performance study of the CT scanner. The Catphan ® phantom is positioned in air in the CT scanner by mounting on the case which placed directly at the end of the table as shown in Figure.3.2.

The Catphan ® 600 phantom is designed so all test sections can be located by precisely indexing the table from center of section 1 (CTP404) to the center of each subsequence test module. The indexing distances from section 1 of Catphan ® 600 test module locations are:

Module Purpose of study	Distance from section 1 center	
CTP404, Slice width, sensitometry and pixel size		
CTP591, Bead geometry	32.5	mm
CTP528, 21 line pair high resolution	70	mm
CTP528, Point source	80	mm
CTP515, Subslice and supra-slice low contrast	110	mm
CTP486, Solid image uniformity module	150	mm
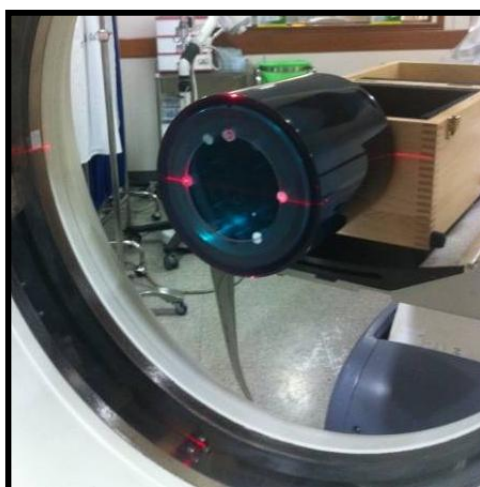
Figure 3.2 Catphan® 600 Phantom**.**
3.6.4 Unfors RaySafe model Xi platinum dosemeter

The Unfors RaySafe Xi platinum (Figure 3.3) is a complete system for multi-parameter measurements on all modalities. The detector is solid state type which is not affected by the temperature and pressure of the environment. The system can be used for the calibration of the radiographic-fluoroscopic, mammography, dental and CT systems with and added option for luminance and illuminance measurements of medical monitors. The Unfors RaySafe Xi platinum prestige is the ultimate QA solution fitted into a small and portable aluminum case. All Unfors RaySafe Xi detectors are interchangeable and function with any base unit.

3.6.5 CT pencil-type ionization chamber

CT pencil-type ionization chamber of 4.9 cm^3 active volume, 10 cm total active length is shown in Fig.3.4. The Unfors RaySafe Xi CT detector is a new hybrid ion chamber designed by Unfors RaySafe. The ion chamber and electronics are combined into one unit making it possible to measure both temperature and pressure to actively compensate for this dependency. The temperature is actually measured inside the ion chamber giving very precise compensations both with and without a CT phantom. With no baseline drift, this carbon fiber ion chamber is ready to use within one minute.

Figure 3.3 Unfors RaySafe model Xi platinum dosimeter

Figure 3.4 The pencil-type ionization Unfors RaySafe Xi CT Detector

Table 3.1 Characteristics of Unfors RaySafe model Xi platinum dosimeter

Unfors RaySafe Xi CT detector	
Unfors RaySafe Xi base unit firmware 4.0 or higher	
Size detector	200 x 20 x 12 mm (7.9 x 0.8 x 0.5 inch)
Size diameter detector	7.5 mm (0.30 inch)
Size diameter phantom adapter	12.5 mm (0.49 inch)
Effective length	100 mm (3.94 inch)
Weight	50 g (1.75 oz)
Range	10 μGy – 9999 Gy (1 mR – 9999R)
	20 μGy/s – 100 mGy/s (140 – 680 R/min)
Uncertainty	5% (at 80 -150 kV; RQR and RQA qualities)
Radial uniformity	$\pm$ 2%
Axial uniformity	$\pm$ 3%, within rated length
Influence of relative humidity	< 0.3% (for RH < 80%) Uncertainty in temp.
	and pressure correction 2%
Pressure range	80.0 – 106.0 kPa
International standard	Fulfill requirements in IEC 61674

3.6.6 Patient

Pediatric patients underwent head computed tomography examination at Faculty of Medicine Siriraj Hospital in July – December 2011 had been divided according to age into 4 groups following IAEA protocol. The study is retrospective. An incomplete radiation data were not included in this study.

3.7 Methods

3.7.1 Perform the quality control of CT GE LightSpeed VCT

The quality control of CT GE LightSpeed VCT was performed following IAEA Human Health series No.19 [19] and ImPACT information leaflet 1: CT scanner acceptance testing version 1.02 [20]. The quality control program consists of the test of performance of electromechanical components, image quality and radiation dose.

3.7.2 Verification of CTDI$_{vol}$ and DLP

The CTDI$_{vol}$ and DLP displayed on the monitor of the console of 64 slice CT had been verified by the comparison of the measurement, the displayed and ImPACTSCAN values. The procedures are as the followings:

- Insert the pencil ionization chamber in the 16 and 32 cm diameter of PMMA phantom. The positioning of the phantom and chamber were investigated to avoid the alignment errors.
- Computed Tomography Dose Index (CTDI) and Dose Length Product (DLP) were recorded from CT monitor and dosimeter readout, where the chamber was inserted at the center and the peripheral positions in phantom. The phantom was scanned three times for each kVp setting.
- The acquisition parameters were 5.0 mm. collimation, 1.0 sec rotation time and 100 mAs. The CTDI$_{vol}$ and DLP that displayed on CT console were recorded after running the scan.
- The data shown on dosimeter was recorded for the calculation of CTDI$_{vol}$ and compared to the displayed data on CT monitor and the ImPACTSCAN values for each kVp.

3.7.3 Study in pediatric patient on head CT

The radiation dose in pediatric patients head CT at Imaging Center Department of Radiology Faculty of Medicine Siriraj Hospital is studied. Collect all data for any consecutive period of time. An incomplete radiation dose data will not be included in this study. Patients with other parameters setting resulting in higher dose than routine protocol will be excluded.

Pediatric patients had been divided into 4 age groups following IAEA protocol

Group 1	Newborn to 1 year $(>0-1)$
Group 2	over 1 to 5 years $(>1-5)$
Group 3	over 5 to 10 years $(>5-10)$
And Group 4	over 10 to 15 years $(>10-15)$

Table 3.2 Parameter setting in each age group.

Age (year)	kVp	mA	mAs*
0 - 1	100	100	50
> 1 - 5	100	150	75
> 5 - 10	120	150	75
> 10 - 15	120	180	90

* Same rotation time in all groups equal 0.5 second.

3.7.4 Data recording

Record the patient's information such as scanning parameters, $CTDI_{vol}$ and DLP in case record form.

3.7.5 Effective dose calculation

Calculate effective dose in each CT scanning parameters from the equation:

Effective dose = DLP x conversion coefficient

The conversion coefficients for head depend on age groups as shown in Table 3.3.

Table 3.3 Conversion coefficient for effective dose calculation

Age	Conversion coefficient $(mSv \cdot mGy^{-1} \cdot cm^{-1})$
0 year	0.0110
1 year	0.0067
5 year	0.0040
10 year	0.0032

3.7.6 Organ dose determination

Determine organ dose in brain, lens, salivary glands, skin and thyroid by ImPACTSCAN software according to ICRP 103.

3.7.7 Risk estimation

Effective dose in each CT scan is calculated from the above equation. Radiation risk in pediatric patients has been estimated for stochastic effect from effective dose in form of numeric ratio per population. Organ dose had been determined for brain, lens, salivary glands, skin and thyroid by ImPACTSCAN software according to ICRP 103.

3.8 Sample size

Primary outcome is continuous data. The sample population is independence, retrospective data. So the sample size is determined by formula;

$$N = (Z_{\alpha/2})^2 \sigma^2/d^2$$
$$= (1.96)^2(0.1)^2/ (0.02)^2$$
$$= 96 \text{ cases}$$

By
α = 0.05
$Z_{\alpha/2}$ = 1.96
d = Acceptable error (0.02)
σ = Variance (0.1) is variable for radiation dose measurement.
σ^2, d are obtained from literature review [16]

3.9 Limitations

For the ImPACT CT Dosimetry Calculator some radiation dose cannot be determined directly. Average radiation dose at approximately location of the organ will be obtained.

3.10 Statistical analysis

3.10.1 Mean and Median will be used for calculation of the patient radiation dose at the highest frequency.

3.10.2 Standard Deviation will be used to refer to variance of data in our study.

3.10.3 Minimum and maximum will represent the lowest and highest values in each range of age.

3.11 Data Collection

3.11.1 Patient information: age, gender and weight.

3.11.2 Scanning parameters: kVp, mA, rotation time, pitch, scan type, slice thickness and scan length.

3.11.3 The $CTDI_{vol}$ and DLP read out from CT monitor.

3.11.4 Organ dose calculated by ImPACTSCAN software.

This data will be collected at Computed Tomography room No.1, Imaging Center, Department of Radiology, Faculty of Medicine Siriraj Hospital, Bangkok Thailand, using 64 Slices GE Lightspeed VCT.

3.12 Data Analysis

The verification of $CTDI_{vol}$ will be reported as percentage difference between the displayed, the measured and the ImPACTSCAN values for each kVp setting. The correction factors will be calculated if the percent differences are greater than 10., The radiation dose data for specific parameter setting will be collected from $CTDI_{vol}$ and DLP displayed on the CT console in the unit of mGy and mGy.cm, respectively, presented in form of table and chart.

Data from pediatric patients will be reported as mean and range as presented in form of table.

The data of $CTDI_{vol}$ and DLP displayed on CT console will be obtained for the calculation of the effective dose for pediatric head CT examination and presented in form of table and bar chart.

Calculated organ dose in brain, lens, salivary glands, skin and thyroid by ImPACTSCAN software according to ICRP 103 will be presented in form of table and bar chart.

Estimated radiation risk in pediatric patients for stochastic effect from effective dose and deterministic effect from organ dose will be presented in form of numeric ratio per population and graph.

3.13 Outcomes

3.13.1 Main outcome: The primary outcome is radiation dose, mGy. DLP value from PACs will be multiplied by the conversion coefficient to obtain the effective dose to determine the stochastic risk from pediatric head CT examination.

3.13.2 Secondary outcome: Organ doses in pediatric patient for the brain, eye lens, salivary glands, thyroid and skin will be evaluated according to ICRP 103 by ImPACTSCAN software and would also be useful for the estimation of deterministic risks in pediatric head CT examinations.

3.14 Expected Benefits

The protocol of head examination in pediatric patient with acceptable radiation dose will be set for reducing radiation risk. This study will lead to the organ doses in the scan area undergoing head CT examination and radiation risk in critical organs of pediatric patient.

3.15 Ethical consideration

Respect for person: This study is a retrospective analysis of patient data which is not involved in the diagnosis and treatment of patients. The acquisition of examination and the corresponding parameters must be accepted by the patient earlier.

Beneficence/Non-maleficence: The patient had already been performed the CT examination to obtain the clinical diagnosis. The result of this research will be benefit to the future study in pediatric to obtain the reduced dose with enough information for the diagnosis. . However, the potential risk to the patient is a patient's confidentiality may be disclosed. The researcher will maintain confidentiality of patient record form in a data identifier that identifies a patient. The data of all patients will be kept confidential.

Justice: The collected data starts from June to December 2011 until reaching the amount of the target population.

The retrospective patient data will be collected after the approval of the ethic committee of Faculty of Medicine, Chulalongkorn University and Faculty of Medicine Siriraj Hospital, Mahidol University. This research is the study of the radiation dose of head CT in pediatric patients with clinical indications. The patients were routinely sent for head CT at Department of Radiology, Siriraj Hospital. The data will be recorded from the PACs system of the hospital.

CHAPTER IV

RESULT

4.1 Quality control of the CT scanner: GE LightSpeed VCT

The quality control of CT scanner was performed following IAEA Human Health series No.19 [19] and ImPACT Information Leaflet [20]. The results include the test of electromechanical component, image quality and radiation dose as shown in Table 4.1 and in Appendix B with the summarized report of CT scanner performance test.

Table 4.1 Report of CT system performance

Location	Imaging Center, Siriraj Hospital
Date of Test	6 April 2012
Room Number	CT1
Manufacturer	GE
Model	LightSpeed VCT

Pass	Scan Localization Light Accuracy
Pass	Alignment of Table to Gantry
Pass	Table Increment Accuracy
Pass	Slice Increment Accuracy
Pass	Gantry Angle Tilt
Pass	Position Dependence and SNR of CT Numbers
Pass	Reproducibility of CT Numbers
Pass	mAs Linearity
Pass	Linearity of CT Numbers
Pass	Accuracy of Distance Measurement
Pass	Image uniformity
Pass	High Contrast Resolution
Pass	Low Contrast Delectability
Pass	Slice Thickness Accuracy

4.2 Verification of Computed Tomography Dose Index (CTDI)

4.2.1 CTDI$_{100}$ in air

The CTDI$_{100}$ in air was measured using head and body protocols and the 100 mm pencil chamber was set at the isocenter of the CT gantry. The scan parameter was 100 mA tube current, 1 sec scan time setting for all measurements at kilovoltage setting of 80, 100, 120 and 140. The results of CTDI in air were shown in Table 4.2 and 4.3.

Table 4.2 The measured CTDI$_{100}$ (mGy) in air for head protocol for each kVp compared to the data from ImPACTSCAN with the percent difference.

kVp	Meter reading	ImPACT	%difference
80	14.73	14.83	0.67
100	23.82	24.23	1.69
120	34.16	35.0	2.4
140	45.62	46.94	2.81

Table 4.3 The measured CTDI$_{100}$ (mGy) in air for body protocol for each kVp compared to the data from ImPACTSCAN with the percent difference.

kVp	Meter reading	ImPACT	%difference
80	14.76	14.83	0.47
100	23.87	24.23	1.49
120	34.17	35.0	2.37
140	45.68	46.94	2.68

4.2.2 CTDI$_{100}$ in head phantom

The CTDI$_{100}$ in head phantom was determined by using a 100 mm pencil ionization chamber placed in each hole of 16 cm diameter PMMA phantom at the isocenter of the CT gantry. The scan parameters were 100 mA, 1 sec scan time, 250 mm FOV for all measurements at each kVp setting of 80, 100, 120 and 140. The result of CTDI in head phantom is shown in Table 4.4.

Table 4.4 The measured CTDI$_{100}$ at each position of head phantom for each kVp.

kVp	CTDI$_{100}$ in head phantom (mGy)					
	At center	At periphery				
		North	East	West	South	Average
80	7.025	12.804	11.690	11.581	10.485	11.640
100	15.299	19.158	17.310	17.123	15.747	17.335
120	23.113	26.328	25.867	25.749	24.319	25.566
140	31.186	36.703	33.032	33.300	30.932	33.492

4.2.3 CTDI$_{100}$ in body phantom

The CTDI$_{100}$ in body phantom was determined by using a 100 mm pencil ion chamber placed in each hole of 32 cm diameter PMMA phantom at the isocenter of the CT gantry. The scan parameters were 100 mA, 1 sec scan time, 360 mm FOV for all measurements at each kVp setting of 80, 100, 120 and 140. The result of CTDI in body phantom is shown in Table 4.5 **.**

Table 4.5 The measured CTDI$_{100}$ at each position of body phantom for each kVp.

kVp	CTDI$_{100}$ in body phantom (mGy)					
	At center	At peripheral				
		North	East	West	South	Average
80	1.772	4.977	4.653	4.824	4.056	4.627
100	3.644	8.327	8.139	8.020	7.367	7.963
120	6.143	13.273	12.475	12.655	11.020	12.356
140	9.901	18.237	17.400	17.803	16.312	17.438

4.2.4 CTDI$_{vol}$ of monitor and calculated CTDI$_w$

Determine the CTDI$_w$ using the results in Table 4.4 and 4.5. The CTDI$_{vol}$ displayed on CT monitor were recorded to compare percentage difference of the calculated values with ImPACT as shown in Table 4.6 and the monitor displayed values with ImPACT as shown in Table 4.7 for CTDI$_{vol}$ in head phantom and Table 4.8 and 4.9 for CTDI$_{vol}$ in body phantom.

Table 4.6 CTDI$_{vol}$ from the calculated CTDI$_w$ and the ImPACT using head protocol 100 mAs and FOV 250 mm.

kVp	CTDI$_{vol}$ (mGy) in head phantom		
	Calculated	ImPACT	% difference
80	10.10	9.40	7.45
100	16.66	16.68	-0.12
120	24.75	25.27	-2.06
140	32.72	34.72	-5.76

Table 4.7 CTDI$_{vol}$ from the monitor and the ImPACT using head protocol 100 mAs and FOV 250 mm.

kVp	CTDI$_{vol}$ (mGy) in head phantom		
	Displayed	ImPACT	% difference
80	6.23	9.40	-33.72
100	12.46	16.68	-25.30
120	20.10	25.27	-20.46
140	28.14	34.72	-18.95

Table 4.8 CTDI$_{vol}$ from the calculated CTDI$_w$ and the ImPACT using body protocol 100 mAs and FOV 360 mm.

kVp	CTDI$_{vol}$ (mGy) in body phantom		
	Calculated	ImPACT	% difference
80	3.68	3.54	3.76
100	6.52	6.83	-4.48
120	10.29	10.87	-5.39
140	14.93	15.57	-4.14

Table 4.9 CTDI$_{vol}$ from the monitor and the ImPACT using body protocol 100 mAs and FOV 360 mm.

kVp	CTDI$_{vol}$ (mGy) in body phantom		
	Displayed	ImPACT	% difference
80	3.18	3.54	-10.22
100	6.37	6.83	-6.72
120	10.27	10.87	-5.53
140	14.38	15.57	-7.64

The discrepancy between CTDI$_{vol}$ from the monitor and the ImPACT are greater than 10 percent. Therefore, the correction factor must be used to apply. Table 4.10 shows the correction factor apply for CTDIvol displayed on monitor in head protocol.

Table 4.10 CTDI$_{vol}$ (mGy) from the monitor, the ImPACT, % difference and correction factor for head protocol.

kVp	Monitor Display	ImPACT	% difference	Correction factor
80	6.23	9.40	-33.72	1.5088
100	12.46	16.68	-25.30	1.3387
120	20.10	25.27	-20.46	1.2572
140	28.14	34.72	-18.95	1.2338

4.3 Patient information and scanning parameters

145 patients were divided into 4 age groups following IAEA protocol. The patient data were shown in Table 4.7

Table 4.11 Patient information in group I from forty-nine patients who underwent head CT examination.

Case No.	In/Out*	Gender	Age		Diagnosis	Examination
			year	month		
1	Out	female		4	Intracranial vascular anomalies	Brain IV
2	In	female	1		F/U HCP	Brain NC
3	Out	male		1	Lt focal seizure	Brain IV
4	Out	male		5	F/U Acute subdural hematoma	Brain NC
5	In	female		3	Retinoblastoma both eyes	Brain IV
6	Out	female		1	Generalized tonic clonic seizure	Brain IV
7	In	male		1	Rt. Adrenocortical tumor	Brain IV
8	Out	male		5	Child abuse&Subdural hematoma	Brain NC
9	In	female		11	R/O Intracranial lesion	Brain IV
10	Out	female		8	HCP	Brain NC
11	In	female		6	Congenital skull mass	Brain IV
12	Out	male		2d	Seizure in 1st day life R/O ICH	Brain NC
13	In	male		6	R/O Intracranial lesion	Brain IV
14	In	male		2	R/O HCP	Brain NC
15	In	female		2	R/O Infected shunt	Brain IV
16	Out	female		10	Head injury	Brain NC
17	Out	female		5	Accident R/O ICH	Brain NC

Table 4.11 Patient information in group I from forty-nine patients who underwent head CT examination. (cont.)

Case No.	In/Out*	Gender	Age year	Age month	Diagnosis	Examination
18	In	male		8	Meningitis	Brain IV
19	Out	male		1	Meningitis	Brain IV
20	Out	female		11	Rt. Focal seizure	Brain IV
21	In	male		9	Salmonella meningitis	Brain IV
22	Out	female		11	R/O Intracranial lesion	Brain IV
23	Out	female		8	R/O HCP	Brain NC
24	In	male		5	Head injury	Brain NC
25	In	female		1	Microcephaly	Brain NC
26	Out	female		1	Accident R/O ICH	Brain NC
27	In	male		4	HCP	Brain NC
28	In	female		1	Preterm neonate	Brain IV
29	Out	male		7	2nd Episode seizure	Brain IV
30	In	male		9	HCP	Brain NC
31	Out	female		65d	R/O ICH	Brain NC
32	In	male		5	R/O brain anomaly	Brain IV
33	Out	male		1d	R/O Intracranial lesion	Brain IV
34	In	female		39d	Prenatal ventriculomegaly	Brain IV
35	Out	female		20d	Cause of microcephaly	Brain IV
36	In	female		7	R/O Bilateral optic atrophy	Brain IV
37	In	female		5	Evaluate tuberouse sclerosis	Brain IV

Table 4.11 Patient information in group I from forty-nine patients who underwent head CT examination. (cont.)

Case No.	In/Out*	Gender	Age		Diagnosis	Examination
			year	month		
38	In	male		7	F/U Meningitis	Brain IV
39	In	female		2	F/U HCP	Brain IV
40	Out	male		1d	R/O Neonatal stroke	Brain NC
41	In	male		8	F/U HCP	Brain NC
42	In	female		1	Evaluate HCP	Brain NC
43	In	female	1		Evaluate complication of meningitis	Brain NC
44	Out	male		5	CNS infection	Brain IV
45	In	female		26d	Microcephaly	Brain IV
46	In	male		6	CNS infection	Brain NC
47	Out	female		10	Evaluate intracranial lesion	Brain IV
48	In	male		6	Evaluate intracranial lesion	Brain IV
49	In	female		1d	Congenital HCP	Brain NC

*In office hours / Outside of office hours

Table 4.12 Patient information in group II from forty patients who underwent head CT examination.

Case No.	In/Out	Gender	Age year	Age month	Diagnosis	Examination
1	In	male	2	5	Choroid plexus papilloma; HCP	Brain NC
2	In	male	4	6	Congenital rotatory nystagmus	Brain IV
3	Out	male	2	0	GBS meningitis	Brain IV
4	In	male	1	8	Obstructive HCP	Brain NC
5	In	female	4	0	Asthma, Lt focal seizure	Brain IV
6	In	male	4	8	Scaly mass	Brain IV
7	Out	male	1	8	Evaluate HCP	Brain NC
8	Out	male	3	3	R/O Neuroblastoma + brain metastasis	Brain IV
9	Out	female	4	2	Leukokoria at lt.eye	Brain IV
10	In	male	4	10	Evaluate HCP	Brain NC
11	In	female	1		F/U HCP	Brain NC
12	In	male	1	9	R/O Intracranial lesion	Brain IV
13	Out	male	1	8	Rt. partial seizure	Brain IV
14	In	male	2	3	Spastic cerebral palsy	Brain IV
15	In	male	3	7	F/U HCP	Brain NC
16	In	male	1	5	Global delayed development	Brain NC
17	In	male	2	3	Tuberous sclerosis	Brain IV
18	In	male	1	3	Non-ketotic hypoglycemia	Brain IV
19	Out	female	3	11	Pfelffer's syndrome	Brain NC
20	In	male	3		Rt.extremity splastic tone & hemi	Brain IV

Table 4.12 Patient information in group II from forty patients who underwent head CT examination. (cont.)

Case No.	In/Out	Gender	Age		Diagnosis	Examination
			year	month		
21	In	female	1	9	Microcephaly	Brain NC
22	In	female	4	5	Epidural hematoma	Brain NC
23	Out	male	1	4	Head injury	Brain NC
24	In	female	1	1	Obstructive HCP	Brain NC
25	Out	male	2		Head injury	Brain NC
26	Out	female	2		Accident R/O ICH	Brain NC
27	Out	female	3	10	Meningocele with HCP	Brain NC
28	In	female	4	2	Accident R/O ICH	Brain NC
29	Out	male	3	7	R/O ICH	Brain NC
30	In	male	3	10	Venous sinus thrombosis	Brain IV
31	Out	male	3		Heart block	Brain IV
32	In	female	4		Evaluate HCP	Brain NC
33	In	male	2	10	R/O ICH	Brain NC
34	In	female	1	11	F/U VP shunt	Brain NC
35	In	male	1	1	Chronic granulomatous with TB meningitis	Brain IV
36	Out	female	4	9	R/O ICH	Brain NC
37	In	male	1	1	Evaluate pituitary damage	Brain IV
38	In	male	3	3	R/O Brain atrophy	Brain NC
39	In	male	2		Retinoblastoma both eyes	Brain IV
40	In	male	3	5	R/O Intracranial tumor	Brain IV

Table 4.13 Patient information in group III from twenty-nine patients who underwent head CT examination.

Case No.	In/Out	Gender	Age year	Age month	Diagnosis	Examination
1	In	female	9	4	Accident R/O ICH	Brain NC
2	In	female	8	10	Seizure, status epilepticus 1 day	Brain IV
3	In	male	7	8	Suprasellar mass	Brain IV
4	Out	female	5	1	Head injury	Brain NC
5	In	female	8	8	W/U Lt. Hemiparesis	Brain IV
6	In	male	8	9	Head injury	Brain NC
7	Out	male	7		Head injury	Brain NC
8	In	female	5	1	Subependymal giant cell astrocytoma	Brain IV
9	In	male	6		Near downing	Brain NC
10	Out	male	6		F/U Comatose	Brain NC
11	Out	male	8	5	Accident R/O ICH	Brain NC
12	In	male	5	11	R/O Brain tumor	Brain IV
13	In	female	5	9	Actinomycetes brain abscess	Brain IV
14	Out	male	5	11	Accident R/O ICH	Brain NC
15	Out	female	6	9	Accident R/O ICH	Brain NC
16	In	female	9	3	Skull lesion at Rt. Temporel area	Brain IV
17	In	female	8	5	Abnormal visual acuity	Brain IV
18	In	male	9	3	HCP	Brain NC
19	Out	male	6	8	R/O ICH	Brain NC

Table 4.13 Patient information in group III from twenty-nine patients who underwent head CT examination. (cont.)

Case No.	In/Out	Gender	Age year	Age month	Diagnosis	Examination
20	Out	male	6	8	F/U ICH	Brain NC
21	Out	male	8	11	Hunter syndrome	Brain NC
22	In	female	5	5	Cardiac arrest & Status epilepticus	Brain NC
23	In	female	7	9	Head injury	Brain NC
24	In	male	9	2	GBM	Brain IV
25	In	male	6	4	F/U Acute subdural hematoma	Brain NC
26	In	male	6	7	Cerebellar vermis tumor	Brain IV
27	In	male	9		Hodgkin's lymphoma	Brain NC
28	In	male	9	10	Congenital macrocephaly	Brain IV
29	In	male	8	10	Evaluate HCP	Brain NC

Table 4.14 Patient information in group IV from twenty-seven patients who underwent head CT examination.

Case No.	In/Out	Gender	Age year	Age month	Diagnosis	Examination
1	In	female	11	7	R/O CNS infection	Brain IV
2	In	male	11	6	F/U HCP	Brain NC
3	Out	male	12	8	Evaluate HCP	Brain NC
4	In	female	12	2	Craniopharyngioma	Brain IV
5	In	female	11	8	Mental retardation	Brain IV
6	Out	male	12	8	Pineal gland tumor	Brain NC

Table 4.14 Patient information in group IV from twenty-seven patients who underwent head CT examination. (cont.)

Case No.	In/Out	Gender	Age		Diagnosis	Examination
			year	month		
7	Out	female	12	3	Craniopharyngioma	Brain NC
8	In	male	13	2	Head injury	Brain NC
9	In	female	14	1	R/O Intracranial mass	Brain IV
10	In	female	12	3	Cerebellum medulloblastoma	Brain IV
11	Out	male	13	4	HCP	Brain NC
12	In	female	11	7	HCP	Brain NC
13	In	female	11	6	Juvenile ossifying fibroma at Lt. orbit	Brain IV
14	In	female	14	11	Pilocytic astrocytoma of optic nerve	Brain IV
15	Out	female	11	6	F/U HCP	Brain NC
16	In	male	11	9	Head injury	Brain NC
17	In	male	12	2	F/U HCP	Brain NC
18	In	male	13		Evaluate infection	Brain NC
19	Out	female	10	11	R/O Encephalitis	Brain IV
20	In	female	10	6	SLE	Brain IV
21	In	male	13		Pineal germinoma	Brain NC
22	In	female	12		Focal seizure	Brain IV
23	In	female	14		Pineal gland tumor with tumor removal	Brain NC
24	In	male	13		Falling from train; Drawsiness	Brain NC
25	In	female	12		Craniopharyngioma with HCP	Brain NC
26	In	male	12		Dysembryoplastic neuroepithelial tumor	Brain IV
27	In	male	11		Head injury; R/O ICH	Brain NC

145 patients were divided into 4 age groups following IAEA protocol. The number of patients in each age group are shown Figure 4.1. Figure 4.2 shows the number of patients in each age group studied between in and out of office hours. Figure 4.3 shows the number of patients without and with contrast in each age group.
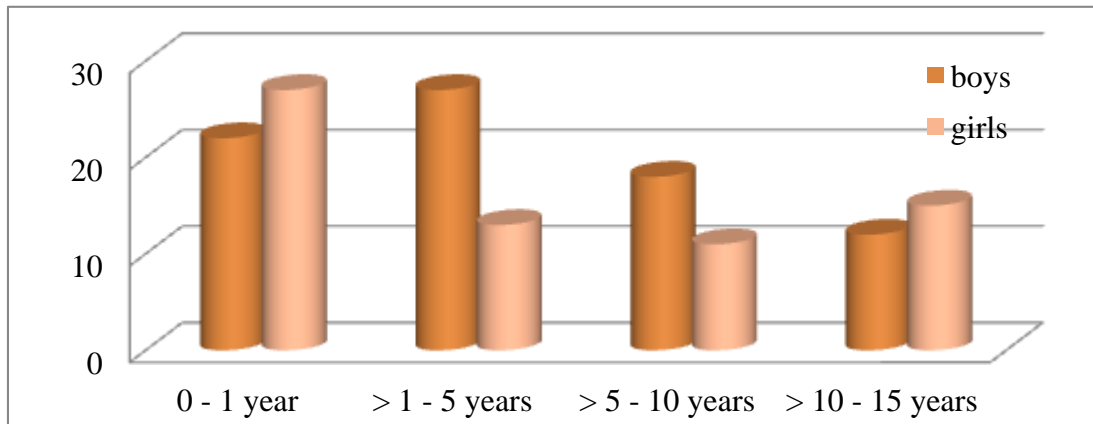
Figure 4.1 Number of patients in each age group divided by gender.
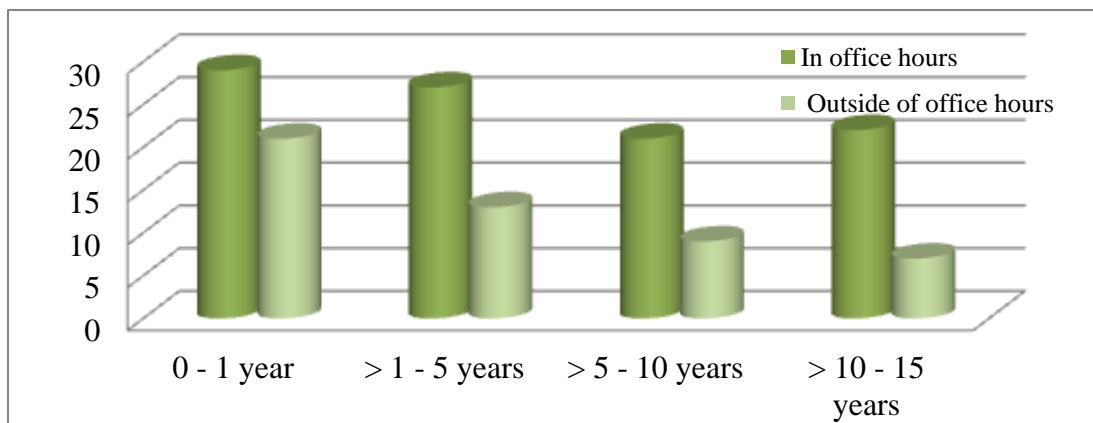
Figure 4.2 Number of patients in each age group studied between in and out of office hours.
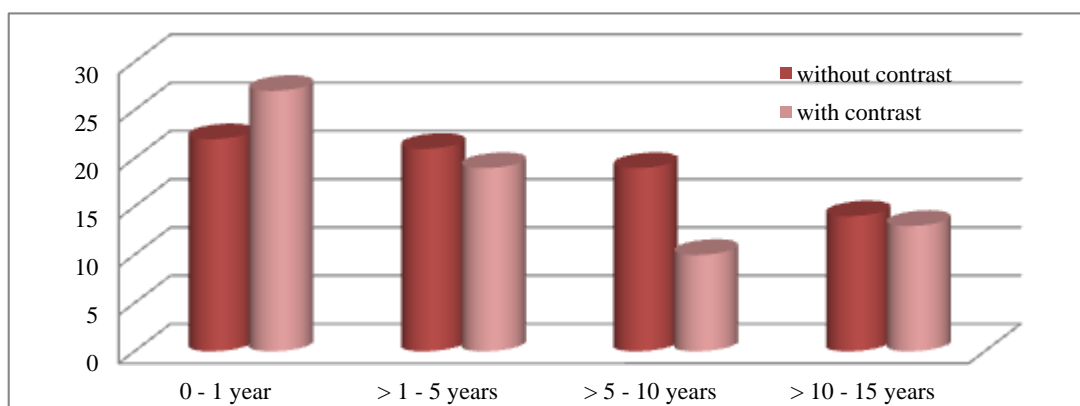
Figure 4.3 Number of patients in each age group with and without contrast media

Table 4.15 Scanning parameter in group I

Case No.	Phase	Scan type	kVp	mA	t_{rot}	Pitch	THK	S_{Coll}	Scan length (mm)	Phase	Scan type	kVp	mA	t_{rot}	Pitch	THK	S_{Coll}	Scan length (mm)
1	1	axial	100	100	0.5	0.969:1	5	20	138.55	2	axial	100	100	0.5	0.969:1	5	20	138.55
2	1	axial	100	100	0.5	0.969:1	5	20	135									
3	1	axial	100	100	0.5	0.969:1	5	20	130.24	2	axial	100	100	0.5	0.969:1	5	20	130.24
4	1	axial	100	100	0.5	0.969:1	5	20	135									
5	1	axial	100	100	0.5	0.969:1	5	20	106	2	axial	100	100	0.5	0.969:1	5	20	106
6	1	axial	100	100	0.5	0.969:1	5	20	117.15	2	axial	100	100	0.5	0.969:1	5	20	117.15
7	1	axial	100	100	0.5	0.969:1	5	20	118.78	2	axial	100	100	0.5	0.969:1	5	20	118.78
8	1	axial	100	100	0.5	0.969:1	5	20	144.59									
9	1	axial	100	100	0.5	0.969:1	5	20	115.86	2	axial	100	100	0.5	0.969:1	5	20	115.86
10	1	axial	100	100	0.5	0.969:1	5	20	155.61									
11	1	helical	100	100	0.5	0.969:1	5	20	140	2	helical	100	100	0.5	0.969:1	5	20	140
12	1	helical	100	100	0.5	0.969:1	5	20	105									

Table 4.15 Scanning parameter in group I (cont.)

Case No.	Phase	Scan type	kVp	mA	t_{rot}	Pitch	THK	S_{Coll}	Scan length (mm)	Phase	Scan type	kVp	mA	t_{rot}	Pitch	THK	S_{Coll}	Scan length (mm)
13	1	axial	100	100	0.5	0.969:1	5	20	118.27	2	axial	100	100	0.5	0.969:1	5	20	118.27
14	1	axial	100	100	0.5	0.969:1	5	20	124.03									
15	1	helical	100	100	0.5	0.969:1	5	20	135	2	helical	100	100	0.5	0.969:1	5	20	135
16	1	axial	100	100	0.5	0.969:1	5	20	155									
17	1	axial	100	100	0.5	0.969:1	5	20	115.54									
18	1	helical	100	100	0.5	0.969:1	5	20	145	2	helical	100	100	0.5	0.969:1	5	20	135
19	1	axial	100	100	0.5	0.969:1	5	20	120.23	2	axial	100	100	0.5	0.969:1	5	20	120.23
20	1	axial	100	100	0.5	0.969:1	5	20	116.78	2	axial	100	100	0.5	0.969:1	5	20	116.78
21	1	axial	100	100	0.5	0.969:1	5	20	72	2	axial	100	100	0.5	0.969:1	5	20	72
22	1	axial	100	100	0.5	0.969:1	5	20	115.74	2	axial	100	100	0.5	0.969:1	5	20	115.74
23	1	axial	100	100	0.5	0.969:1	5	20	135.51									
24	1	axial	100	100	0.5	0.969:1	5	20	135									
25	1	axial	100	100	0.5	0.969:1	5	20	97.49									
26	1	axial	100	100	0.5	0.969:1	5	20	115									

Table 4.15 Scanning parameter in group I (cont.)

Case No.	Phase	Scan type	kVp	mA	t_{rot}	Pitch	THK	S_{Coll}	Scan length (mm)	Phase	Scan type	kVp	mA	t_{rot}	Pitch	THK	S_{Coll}	Scan length (mm)
27	1	axial	100	100	0.5	0.969:1	5	20	137.30									
28	1	axial	100	100	0.5	0.969:1	5	20	104.4	2	axial	100	100	0.5	0.969:1	5	20	104.4
29	1	axial	100	100	0.5	0.969:1	5	20	118.27	2	axial	100	100	0.5	0.969:1	5	20	118.27
30	1	axial	100	100	0.5	0.969:1	5	20	176.6									
31	1	axial	100	100	0.5	0.969:1	5	20	115									
32	1	axial	100	100	0.5	0.969:1	5	20	120.92	2	axial	100	100	0.5	0.969:1	5	20	120.92
33	1	helical	100	100	0.5	0.969:1	5	20	110	2	helical	100	100	0.5	0.969:1	5	20	110
34	1	axial	100	100	0.5	0.969:1	5	20	96.62	2	axial	100	100	0.5	0.969:1	5	20	96.62
35	1	axial	100	100	0.5	0.969:1	5	20	78.64	2	axial	100	100	0.5	0.969:1	5	20	78.64
36	1	axial	100	100	0.5	0.969:1	5	20	126.38	2	axial	100	100	0.5	0.969:1	5	20	126.38
36	1	axial	100	100	0.5	0.969:1	5	20	126.38	2	axial	100	100	0.5	0.969:1	5	20	126.38
37	1	axial	100	100	0.5	0.969:1	5	20	118.78	2	axial	100	100	0.5	0.969:1	5	20	118.78

Table 4.15 Scanning parameter in group I (cont.)

Case No.	Phase	Scan type	kVp	mA	t_{rot}	Pitch	THK	S_{Coll}	Scan length (mm)	Phase	Scan type	kVp	mA	t_{rot}	Pitch	THK	S_{Coll}	Scan length (mm)
38	1	axial	100	100	0.5	0.969:1	5	20	120.26	2	axial	100	100	0.5	0.969:1	5	20	120.26
39	1	axial	100	100	0.5	0.969:1	5	20	115.54									
40	1	axial	80	100	0.5	0.969:1	5	20	118.27									
41	1	axial	100	100	0.5	0.969:1	5	20	115									
42	1	axial	100	100	0.5	0.969:1	5	20	115									
43	1	axial	100	100	0.5	0.969:1	5	20	115	2	axial	100	100	0.5	0.969:1	5	20	115
44	1	helical	100	50	0.5	0.969:1	5	20	115	2	helical	100	55	0.5	0.969:1	5	20	115
45	1	axial	100	100	0.5	0.969:1	5	20	98.59									
46	1	axial	100	100	0.5	0.969:1	5	20	136	2	axial	100	100	0.5	0.969:1	5	20	136
47	1	axial	100	100	0.5	0.969:1	5	20	119.06	2	axial	100	100	0.5	0.969:1	5	20	119.06
48	1	axial	100	100	0.5	0.969:1	5	20	138.84									
49	1	helical	100	100	0.5	0.969:1	5	20	140									

Table 4.16 Scanning parameter in group II

Case No.	Phase	Scan type	kVp	mA	t_{rot}	Pitch	THK	S_{Coll}	Scan length (mm)	Phase	Scan type	kVp	mA	t_{rot}	Pitch	THK	S_{Coll}	Scan length (mm)
1	**1**	helical	100	150	0.5	0.969:1	5	20	145	**2**	axial	100	150	0.5	0.969:1	5	20	136.88
2	**1**	axial	100	150	0.5	0.969:1	5	20	137.53	**2**	axial	100	150	0.5	0.969:1	5	20	137.53
3	**1**	axial	100	100	0.5	0.969:1	5	20	120	**2**	axial	100	100	0.5	0.969:1	5	20	125
4	**1**	axial	100	100	0.5	0.969:1	5	20	140									
5	**1**	axial	100	150	0.5	0.969:1	5	20	155	**2**	axial	100	150	0.5	0.969:1	5	20	155
6	**1**	axial	100	150	0.5	0.969:1	5	20	144.61	**2**	axial	100	150	0.5	0.969:1	5	20	144.61
7	**1**	axial	100	100	0.5	0.969:1	5	20	156.72									
8	**1**	helical	100	150	0.5	0.969:1	5	20	130	**2**	helical	100	150	0.5	0.969:1	5	20	130
9	**1**	helical	100	150	0.5	0.969:1	5	20	145	**2**	helical	100	150	0.5	0.969:1	5	20	145
10	**1**	axial	100	150	0.5	0.969:1	5	20	155.72									
11	**1**	axial	100	100	0.5	0.969:1	5	20	135									
12	**1**	axial	100	100	0.5	0.969:1	5	20	137.53	**2**	axial	100	100	0.5	0.969:1	5	20	137.53
13	**1**	axial	100	100	0.5	0.969:1	5	20	138.02	**2**	axial	100	100	0.5	0.969:1	5	20	138.02

Table 4.16 Scanning parameter in group II (cont.)

Case No.	Phase	Scan type	kVp	mA	t_{rot}	Pitch	THK	S_{Coll}	Scan length (mm)	Phase	Scan type	kVp	mA	t_{rot}	Pitch	THK	S_{Coll}	Scan length (mm)
14	1	axial	100	150	0.5	0.969:1	5	20	142.36	2	axial	100	150	0.5	0.969:1	5	20	142.36
15	1	helical	100	150	0.5	0.969:1	5	20	120									
16	1	helical	100	100	0.5	0.969:1	5	20	120									
17	1	helical	100	150	0.5	0.969:1	5	20	165	2	helical	100	150	0.5	0.969:1	5	20	165
18	1	axial	100	100	0.5	0.969:1	5	20	155.89	2	axial	100	100	0.5	0.969:1	5	20	155.89
19	1	axial	100	150	0.5	0.969:1	5	20	206.87									
20	1	axial	100	150	0.5	0.969:1	5	20	142	2	axial	100	150	0.5	0.969:1	5	20	142
21	1	helical	100	100	0.5	0.969:1	5	20	130									
22	1	helical	100	150	0.5	0.969:1	5	20	125									
23	1	helical	100	100	0.5	0.969:1	5	20	140									
24	1	axial	100	100	0.5	0.969:1	5	20	115									
25	1	axial	100	150	0.5	0.969:1	5	20	135									
26	1	axial	100	150	0.5	0.969:1	5	20	135									
27	1	axial	100	150	0.5	0.969:1	5	20	159.4									

Table 4.16 Scanning parameter in group II (cont.)

Case No.	Phase	Scan type	kVp	mA	t_{rot}	Pitch	THK	S_{Coll}	Scan length (mm)	Phase	Scan type	kVp	mA	t_{rot}	Pitch	THK	S_{Coll}	Scan length (mm)
28	1	axial	100	150	0.5	0.969:1	5	20	135.63									
29	1	axial	100	150	0.5	0.969:1	5	20	155									
30	1	axial	100	150	0.5	0.969:1	5	20	135.02	2	axial	100	150	0.5	0.969:1	5	20	135.02
31	1	axial	100	150	0.5	0.969:1	5	20	139.13	2	axial	100	150	0.5	0.969:1	5	20	139.13
32	1	axial	100	150	0.5	0.969:1	5	20	118.78									
33	1	axial	100	150	0.5	0.969:1	5	20	145.49									
34	1	axial	100	100	0.5	0.969:1	5	20	135.87									
35	1	axial	100	100	0.5	0.969:1	5	20	138.39	2	axial	100	100	0.5	0.969:1	5	20	138.39
36	1	axial	100	150	0.5	0.969:1	5	20	140									
37	1	helical	100	100	0.5	0.969:1	5	20	127.25	2	helical	100	100	0.5	0.969:1	5	20	127.25
38	1	axial	100	150	0.5	0.969:1	5	20	129.65									
39	1	helical	100	150	0.5	0.969:1	5	20	150	2	helical	100	150	0.5	0.969:1	5	20	150
40	1	axial	100	150	0.5	0.969:1	5	20	144.61	2	axial	100	150	0.5	0.969:1	5	20	144.61

Table 4.17 Scanning parameter in group III

Case No.	Phase	Scan type	kVp	mA	t_{rot}	Pitch	THK	S_{Coll}	Scan length (mm)	Phase	Scan type	kVp	mA	t_{rot}	Pitch	THK	S_{Coll}	Scan length (mm)
1	1	axial	120	150	0.5	0.969:1	5	20	135									
2	1	axial	120	150	0.5	0.969:1	5	20	138.84	2	axial	120	150	0.5	0.969:1	5	20	138.84
3	1	axial	120	150	0.5	0.969:1	5	20	140.1	2	axial	120	150	0.5	0.969:1	5	20	140.1
4	1	axial	100	150	0.5	0.969:1	5	20	144.94									
5	1	axial	120	150	0.5	0.969:1	5	20	135.42	2	axial	120	150	0.5	0.969:1	5	20	135.42
6	1	axial	120	150	0.5	0.969:1	5	20	155									
7	1	axial	120	150	0.5	0.969:1	5	20	155.38									
8	1	axial	100	150	0.5	0.969:1	5	20	167	2	axial	100	150	0.5	0.969:1	5	20	167
9	1	axial	120	150	0.5	0.969:1	5	20	135.13									
10	1	axial	120	150	0.5	0.969:1	5	20	135									
11	1	axial	120	150	0.5	0.969:1	5	20	155									
12	1	axial	100	150	0.5	0.969:1	5	20	135	2	axial	100	150	0.5	0.969:1	5	20	135
13	1	axial	100	100	0.5	0.969:1	5	20	136.5	2	axial	100	100	0.5	0.969:1	5	20	136.5
14	1	axial	120	150	0.5	0.969:1	5	20	155									
15	1	axial	120	150	0.5	0.969:1	5	20	136.68									

Table 4.17 Scanning parameter in group III (cont.)

Case No.	Phase	Scan type	kVp	mA	t_{rot}	Pitch	THK	S_{Coll}	Scan length (mm)	Phase	Scan type	kVp	mA	t_{rot}	Pitch	THK	S_{Coll}	Scan length (mm)
16	1	axial	120	150	0.5	0.969:1	5	20	138.51	2	axial	120	150	0.5	0.969:1	5	20	138.51
17	1	axial	120	150	0.5	0.969:1	5	20	137.47	2	axial	120	150	0.5	0.969:1	5	20	137.47
18	1	axial	120	150	0.5	0.969:1	5	20	165.48									
19	1	axial	120	150	0.5	0.969:1	5	20	136.07									
20	1	axial	120	150	0.5	0.969:1	5	20	135.42									
21	1	axial	120	150	0.5	0.969:1	5	20	157.9									
22	1	axial	100	150	0.5	0.969:1	5	20	136.33									
23	1	axial	120	150	0.5	0.969:1	5	20	135.63									
24	1	helical	120	150	0.5	0.969:1	5	20	175									
25	1	axial	120	150	0.5	0.969:1	5	20	118.15									
26	1	axial	120	150	0.5	0.969:1	5	20	137.5	2	helical	120	150	0.5	0.969:1	5	20	130
27	1	axial	120	150	0.5	0.969:1	5	20	159.08									
28	1	axial	120	150	0.5	0.969:1	5	20	156.34	2	axial	120	150	0.5	0.969:1	5	20	156.34
29	1	axial	120	150	0.5	0.969:1	5	20	135									

Table 4.18 Scanning parameter in group IV

Case No.	Phase	Scan type	kVp	mA	t_{rot}	Pitch	THK	S_{Coll}	Scan length (mm)	Phase	Scan type	kVp	mA	t_{rot}	Pitch	THK	S_{Coll}	Scan length (mm)
1	1	axial	120	180	0.5	0.969:1	5	20	135	2	axial	120	180	0.5	0.969:1	5	20	135
2	1	axial	120	180	0.5	0.969:1	5	20	181.4	2	helical	120	200	0.5	0.969:1	5	20	210
3	1	axial	120	120	0.5	0.969:1	5	20	155	2								
4	1	axial	120	100	0.5	0.969:1	5	20	140	2	axial	120	100	0.5	0.969:1	5	20	140
5	1	axial	120	180	0.5	0.969:1	5	20	143.2	2	axial	120	180	0.5	0.969:1	5	20	143.2
6	1	axial	120	180	0.5	0.969:1	5	20	151.5									
7	1	axial	120	180	0.5	0.969:1	5	20	142.9									
8	1	axial	120	180	0.5	0.969:1	5	20	155									
9	1	axial	120	180	0.5	0.969:1	5	20	175	2	axial	120	180	0.5	0.969:1	5	20	175
10	1	axial	120	180	0.5	0.969:1	5	20	135	2	axial	120	180	0.5	0.969:1	5	20	135
11	1	helical	120	180	0.5	0.969:1	5	20	150									
12	1	axial	120	180	0.5	0.969:1	5	20	135.1									
13	1	helical	120	180	0.5	0.969:1	5	20	155	2	helical	120	180	0.5	0.969:1	5	20	155

Table 4.18 Scanning parameter in group IV (cont.)

Case No.	Phase	Scan type	kVp	mA	t_{rot}	Pitch	THK	S_{Coll}	Scan length (mm)	Phase	Scan type	kVp	mA	t_{rot}	Pitch	THK	S_{Coll}	Scan length (mm)
14	1	axial	120	180	0.5	0.969:1	5	20	135.1	2	axial	120	180	0.5	0.969:1	5	20	135.1
15	1	axial	120	180	0.5	0.969:1	5	20	119.6									
16	1	axial	120	180	0.5	0.969:1	5	20	137.5									
17	1	axial	120	180	0.5	0.969:1	5	20	156.3									
18	1	helical	120	180	0.5	0.969:1	5	20	130									
19	1	axial	120	150	0.5	0.969:1	5	20	136.5	2	axial	120	150	0.5	0.969:1	5	20	136.5
20	1	axial	120	150	0.5	0.969:1	5	20	136.3	2	axial	120	150	0.5	0.969:1	5	20	136.3
21	1	axial	120	180	0.5	0.969:1	5	20	137.3	2	axial	120	180	0.5	0.969:1	5	20	137.3
22	1	axial	120	180	0.5	0.969:1	5	20	135	2	axial	120	180	0.5	0.969:1	5	20	135
23	1	axial	120	180	0.5	0.969:1	5	20	138									
24	1	axial	120	180	0.5	0.969:1	5	20	135.5									
25	1	axial	120	180	0.5	0.969:1	5	20	141.6									
26	1	helical	120	180	0.5	0.969:1	5	20	180	2	helical	120	180	0.5	0.969:1	5	20	180
27	1	helical	120	180	0.5	0.969:1	5	20	150									

4.4 Radiation dose

CTDI$_{vol}$ and DLP were recorded from monitor and the correction factors were applied. To calculate the effective dose, DLP was multiplied by conversion coefficient for Head CT [6].

Table 4.19 Radiation dose data in group I

Case no.	CTDI$_{vol}$ (mGy)		DLP (mGy.cm)		Effective dose (mSv)	
	total	per series	total	per series	total	per series
1	14.35	7.18	154.12	77.06	1.7	0.85
2	7.363	7.36	77.06	77.06	0.85	0.85
3	13.01	6.51	132.1	66.05	1.45	0.73
4	7.363	7.36	77.06	77.06	0.85	0.85
5	14.73	7.36	132.1	66.05	1.45	0.73
6	14.46	7.23	132.1	66.05	1.45	0.73
7	14.27	7.14	132.1	66.05	1.45	0.73
8	6.881	6.88	77.06	77.06	0.85	0.85
9	14.62	7.31	132.1	66.05	1.45	0.73
10	6.827	6.83	77.06	77.06	0.85	0.85
11	15.21	7.6	184.98	92.49	2.03	1.02
12	7.604	7.6	72.61	72.61	0.8	0.8
13	14.32	7.16	132.1	66.05	1.45	0.73
14	6.827	6.83	66.05	66.05	0.73	0.73
15	15.21	7.6	179.3	89.65	1.97	0.99
16	7.363	7.36	88.06	88.06	0.97	0.97
17	7.336	7.34	66.05	66.05	0.73	0.73
18	15.21	7.6	184.98	92.49	2.03	1.02

Table 4.19 Radiation dose data in group I (cont.)

Case no.	CTDI$_{vol}$ (mGy)		DLP (mGy.cm)		Effective dose (mSv)	
	total	per series	total	per series	total	per series
19	14.08	7.04	132.1	66.05	1.45	0.73
20	14.51	7.26	132.1	66.05	1.45	0.73
21	14.73	7.36	154.12	77.06	1.7	0.85
22	14.65	7.32	132.1	66.05	1.45	0.73
23	7.336	7.34	77.06	77.06	0.85	0.85
24	7.363	7.36	77.06	77.06	0.85	0.85
25	7.175	7.18	55.04	55.04	0.61	0.61
26	7.363	7.36	66.05	66.05	0.73	0.73
27	7.242	7.24	77.06	77.06	0.85	0.85
28	13.41	6.71	110.08	55.04	1.21	0.61
29	14.32	7.16	132.1	66.05	1.45	0.73
30	6.854	6.85	88.06	88.06	0.97	0.97
31	7.363	7.36	66.05	66.05	0.73	0.73
32	14	7	132.1	66.05	1.45	0.73
33	15.21	7.6	150.9	75.45	1.66	0.83
34	14.48	7.24	110.08	55.04	1.21	0.61
35	14.06	7.03	88.06	44.03	0.97	0.48
36	13.41	6.71	132.1	66.05	1.45	0.73
37	14.27	7.14	132.1	66.05	1.45	0.73
38	14.08	7.04	132.1	66.05	1.45	0.73
39	7.336	7.34	66.05	66.05	0.73	0.73
40	3.666	3.67	30.04	30.04	0.33	0.33

Table 4.19 Radiation dose data in group I (cont.)

Case no.	CTDI$_{vol}$ (mGy)		DLP (mGy.cm)		Effective dose (mSv)	
	total	per series	total	per series	total	per series
41	6.653	7.36	66.05	66.05	0.73	0.73
42	7.363	7.36	66.05	66.05	0.73	0.73
43	14.73	7.36	132.1	66.05	1.45	0.73
44	14.57	7.28	148.24	74.12	1.63	0.82
45	7.095	7.1	55.04	55.04	0.61	0.61
46	14.73	7.36	154.12	77.06	1.7	0.85
47	14.24	7.12	132.1	66.05	1.45	0.73
48	7.162	7.16	77.06	77.06	0.85	0.85
49	7.604	7.6	92.49	92.49	1.02	1.02

Table 4.20 Radiation dose data in group II

Case no.	CTDI$_{vol}$ (mGy)		DLP (mGy.cm)		Effective dose (mSv)	
	total	per series	total	per series	total	per series
1	22.3	11.15	258.38	129.19	1.73	0.87
2	21.69	10.84	231.16	115.58	1.55	0.77
3	15.21	7.604	165.1	82.55	1.11	0.55
4	7.604	7.604	92.49	92.49	0.62	0.62
5	22.12	11.06	264.2	132.1	1.77	0.89
6	20.64	10.32	231.16	115.58	1.55	0.77
7	7.283	7.283	88.06	88.06	0.59	0.59
8	22.81	11.41	260.42	130.21	1.74	0.87
9	22.81	11.41	286	143	1.92	0.96

Table 4.20 Radiation dose data in group II (cont.)

Case no.	CTDI$_{vol}$ (mGy)		DLP (mGy.cm)		Effective dose (mSv)	
	total	per series	total	per series	total	per series
10	11	11	132.1	132.1	0.89	0.89
11	7.363	7.363	77.06	77.06	0.52	0.52
12	14.46	7.229	154.12	77.06	1.03	0.52
13	14.4	7.202	154.12	77.06	1.03	0.52
14	20.96	10.48	231.16	115.58	1.55	0.77
15	11.41	11.41	121.69	121.69	0.82	0.82
16	7.604	7.604	81.13	81.13	0.54	0.54
17	22.81	11.41	320.08	160.04	2.14	1.07
18	12.77	6.386	154.12	77.06	1.03	0.52
19	10.42	10.42	165.12	165.12	1.11	1.11
20	22.12	11.06	231.16	115.58	1.55	0.77
21	7.604	7.604	86.81	86.81	0.58	0.58
22	11.41	11.41	125.95	125.95	0.84	0.84
23	7.604	7.604	92.49	92.49	0.62	0.62
24	7.363	7.363	66.05	66.05	0.44	0.44
25	11.06	11.06	115.58	115.58	0.77	0.77
26	11.06	11.06	115.58	115.58	0.77	0.77
27	10.75	10.75	132.1	132.1	0.89	0.89
28	11	11	115.58	115.58	0.77	0.77
29	11.06	11.06	132.1	132.1	0.89	0.89
30	22.09	11.04	231.16	115.58	1.55	0.77
31	21.45	10.72	231.16	115.58	1.55	0.77
32	10.7	10.7	99.07	99.07	0.66	0.66

Table 4.20 Radiation dose data in group II (cont.)

Case no.	CTDIᵥₒₗ (mGy)		DLP (mGy.cm)		Effective dose (mSv)	
	total	per series	total	per series	total	per series
33	10.54	10.54	115.58	115.58	0.77	0.77
34	7.323	7.323	77.06	77.06	0.52	0.52
35	14.65	7.323	154.12	77.06	1.03	0.52
36	11.41	11.41	138.74	138.74	0.93	0.93
37	15.21	7.604	160.84	80.42	1.08	0.54
38	9.799	9.799	99.07	99.07	0.66	0.66
39	22.81145	11.41	294.52	147.26	1.97	0.9866
40	20.64275	10.32	231.16	115.58	1.55	0.7744

Table 4.21 Radiation dose data in group III

Case no.	CTDIᵥₒₗ (mGy)		DLP (mGy.cm)		Effective dose (mSv)	
	total	per series	total	per series	total	per series
1	16.75	16.75	186.43	186.43	0.75	0.75
2	32.56	16.28	372.86	186.43	1.49	0.75
3	32.26	16.13	372.86	186.43	1.49	0.75
4	10.6	10.6	99.07	99.07	0.4	0.4
5	33.39	16.7	372.86	186.43	1.49	0.75
6	16.75	16.75	213.06	213.06	0.85	0.85
7	16.7	16.7	213.06	213.06	0.85	0.85
8	20.43	10.21	264.2	132.1	1.06	0.53
9	16.72	16.72	186.43	186.43	0.75	0.75
10	16.75	16.75	186.43	186.43	0.75	0.75

Table 4.21 Radiation dose data in group III (cont.)

Case no.	CTDI$_{vol}$ (mGy)		DLP (mGy.cm)		Effective dose (mSv)	
	total	per series	total	per series	total	per series
11	16.75	16.75	213.06	213.06	0.85	0.85
12	22.12	11.06	231.16	115.58	0.92	0.46
13	20.54	10.27	231.16	115.58	0.92	0.46
14	16.75	16.75	213.06	213.06	0.85	0.85
15	16.72	16.72	186.43	186.43	0.75	0.75
16	33.37	16.68	372.86	186.43	1.49	0.75
17	33.39	16.7	372.86	186.43	1.49	0.75
18	15.68	15.68	213.06	213.06	0.85	0.85
19	16.62	16.62	186.43	186.43	0.75	0.75
20	16.7	16.7	186.43	186.43	0.75	0.75
21	16.43	16.43	213.06	213.06	0.85	0.85
22	10.95	10.95	115.58	115.58	0.46	0.46
23	16.66	16.66	186.43	186.43	0.75	0.75
24	17.29	17.29	271.88	271.88	1.09	1.09
25	16.65	16.65	157.79	157.79	0.63	0.63
26	34.03	17.02	396.45	198.225	1.59	0.79
27	16.31	16.31	213.06	213.06	0.85	0.85
28	33.19	16.6	426.12	213.06	1.7	0.85
29	16.75	16.75	186.43	186.43	0.75	0.75

Table 4.22 Radiation dose data in group IV

Case no.	CTDI$_{vol}$ (mGy)		DLP (mGy.cm)		Effective dose (mSv)	
	total	per series	total	per series	total	per series
1	40.18	20.09	447.42	223.71	1.43	0.72
2	40.36	20.18	675.94	337.97	2.16	1.08
3	20.09	20.09	255.67	255.67	0.82	0.82
4	23.03	11.52	298.36	149.18	0.95	0.48
5	37.87	18.93	447.42	223.71	1.43	0.72
6	20.09	20.09	223.71	223.71	0.72	0.72
7	19.45	19.45	223.71	223.71	0.72	0.72
8	20.09	20.09	255.67	255.67	0.82	0.82
9	40.18	20.09	575.26	287.63	1.84	0.92
10	40.18	20.09	447.42	223.71	1.43	0.72
11	20.73	20.73	285.02	285.02	0.91	0.91
12	20.08	20.08	223.71	223.71	0.72	0.72
13	41.46	20.73	586.52	293.26	1.88	0.94
14	40.13	20.06	447.42	223.71	1.43	0.72
15	19.31	19.31	191.75	191.75	0.61	0.61
16	19.73	19.73	223.71	223.71	0.72	0.72
17	19.91	19.91	255.67	255.67	0.82	0.82
18	20.73	20.73	252.03	252.03	0.81	0.81
19	33.11	16.56	372.86	186.43	1.19	0.6
20	33.16	16.58	372.86	186.43	1.19	0.6
21	39.5	19.75	447.42	223.71	1.43	0.72

Table 4.22 Radiation dose data in group IV (cont.)

Case no.	CTDI$_{vol}$ (mGy)		DLP (mGy.cm)		Effective dose (mSv)	
	total	per series	total	per series	total	per series
22	40.18	20.09	447.42	223.71	1.43	0.72
23	19.65	19.65	223.71	223.71	0.72	0.72
24	20.01	20.01	223.71	223.71	0.72	0.72
25	19.16	19.16	223.71	223.71	0.72	0.72
26	41.46	20.73	669	334.5	2.14	1.07
27	20.73	20.73	285.02	285.02	0.91	0.91

4.4.1. Diagnostic Reference Levels (DRLs)

DRLs is determined with the third quartile of the spread of the median doses of common protocols from a national survey of imaging practice. Provide a method for optimizing the medical procedure and radiation protection of the patients ongoing. The third quartile or 75% of the local dose indicators are below the national DRL; which can estimate that local dose indicators appropriate in demonstrate a good quality practice. For the 25% of local dose indicators which are above the national DRL can be a performance and determine that the corresponding procedure is not fully optimized. In computed tomography, two parameters have also been used to express DRLs are the CTDI$_{vol}$ and DLP. Table 4.23 shows CTDI$_{vol}$ and DLP of this study compare with recommendations from the UK and EU national reference doses for pediatric patients from various age groups. CTDI$_{vol}$ and DLP increase with age; it is clear that at all ages in this study, the CTDI and DLP are far below DRL from UK and EU.

Table 4.23: DRLs (mGy for CTDI and mGy cm for DLP) for different patient groups and examinations and in this research, UK2003, and EU.

Age Group	Quantity	This study	UK 2003	EU
< 1 year	CTDI$_{vol}$	7	30	
	DLP	77	270	300
1-5 years	CTDI$_{vol}$	11	45	
	DLP	130	470	600
5-10 years	CTDI$_{vol}$	17	50	
	DLP	213	620	750
10-15 years	CTDI$_{vol}$	20	65	
	DLP	256	930	
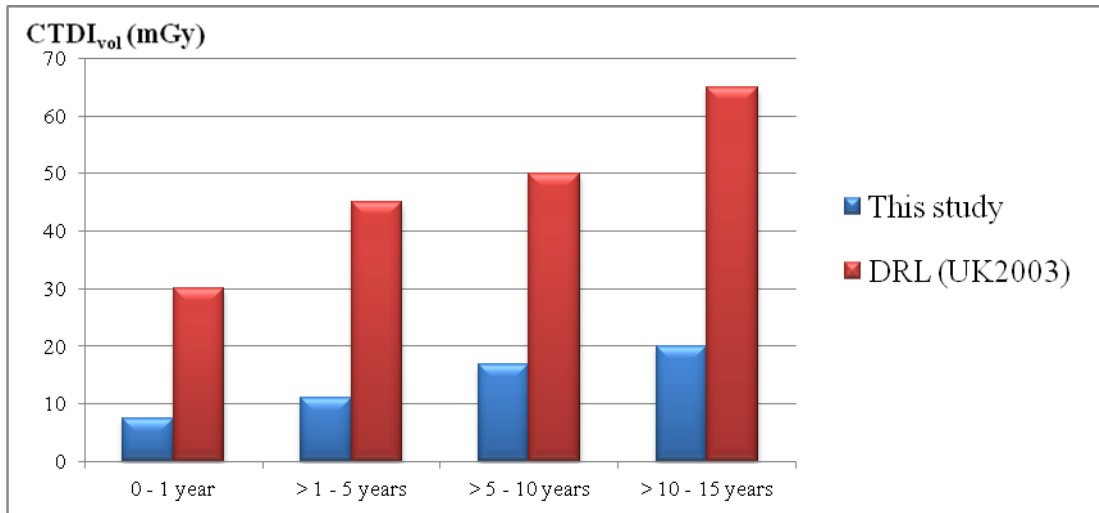
Figure 4.4 Compare 3rd quartile of CTDI$_{vol}$ in this study with DRL (UK2003)
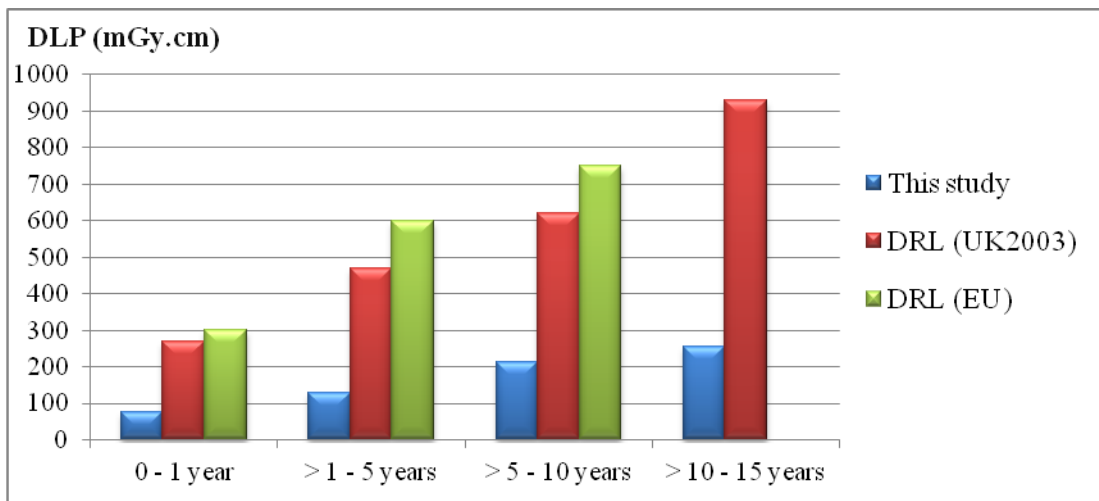
Figure 4.5 Compare 3rd quartile of DLP in this study with DRL UK2003 and EU.
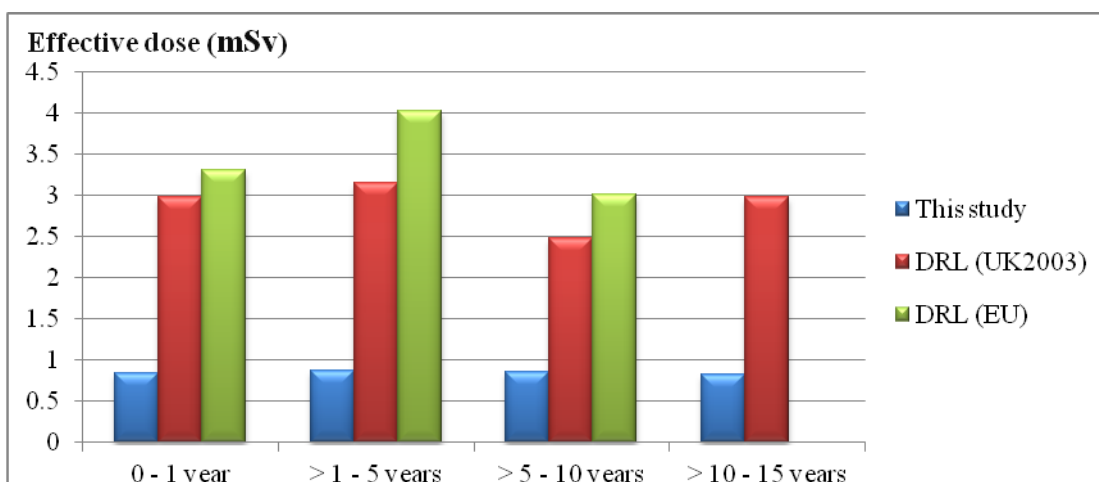
Figure 4.6 Compare 3rd quartile of effective dose in this study with DRL UK and EU.

4.4.2. Organ dose

Determine organ dose in brain, lens, salivary glands, skin and thyroid by **ImPACT CT Patient Dosimetry Calculator Version 1.0.4** according to ICRP 103. Organ dose shown in the table below contains only one series, the cases which scan more than one series can use this value multiplied by number of series.

Table 4.24 Organ dose data in group I

Case No.	Organ dose (mGy per series)				
	brain	lens	salivary gland	skin	thyroid
1	6.5	7.47	6.5	0.46	0.26
2	6.5	7.5	6.5	0.45	0.23
3	6.4	7.4	6.4	0.43	0.2
4	6.5	7.5	6.5	0.45	0.23
5	6.5	4.3	6.5	0.35	0.1
6	6.14	7.14	6.14	0.39	0.14
7	6.18	7.18	6.18	0.4	0.15
8	6.59	7.59	6.59	0.49	0.31
9	6.5	7.12	6.5	0.38	0.13
10	6.61	7.6	6.61	0.52	0.44
11	6.5	7.5	6.5	0.47	0.27
12	5.6	4	5.6	0.35	0.1
13	6.17	7.17	6.17	0.39	0.14
14	6.28	7.28	6.28	0.42	0.17
15	6.5	7.5	6.5	0.45	0.23
16	6.6	7.6	6.6	0.52	0.43
17	6.11	7.11	6.11	0.38	0.13
18	6.6	7.5	6.6	0.49	0.31
19	6.2	7.2	6.2	0.4	0.15

Table 4.24 Organ dose data in group I (cont.)

Case No.	Organ dose (mGy per series)				
	brain	lens	salivary gland	skin	thyroid
20	6.5	7.14	6.5	0.39	0.14
21	6.58	0.51	6.58	0.48	0.08
22	6.11	7.11	6.11	0.38	0.13
23	6.5	7.41	6.5	0.45	0.23
24	6.5	7.5	6.5	0.45	0.23
25	5.25	1.62	5.25	0.33	0.08
26	6.1	7	6.1	0.38	0.13
27	6.5	7.45	6.5	0.46	0.25
28	5.58	3.81	5.58	0.35	0.1
29	6.17	7.17	6.17	0.39	0.14
30	6.8	7.7	6.8	0.6	0.8
31	6.1	7	6.1	0.38	0.13
32	6.22	7.22	6.22	0.4	0.15
33	5.9	5.5	5.9	0.37	0.12
34	5.2	1.35	5.2	0.33	0.08
35	3.89	0.37	3.89	0.27	0.05
36	6.33	7.33	6.33	0.42	0.18
37	6.18	7.18	6.18	0.4	0.15
38	6.21	7.21	6.21	0.4	0.15
39	6.11	7.11	6.11	0.38	0.13
40	3.27	3.77	3.27	0.21	0.07
41	6.1	7	6.1	0.38	0.13
42	6.1	7	6.1	0.38	0.13

Table 4.24 Organ dose data in group I (cont.)

Case No.	Organ dose (mGy per series)				
	brain	**lens**	**salivary gland**	**skin**	**thyroid**
43	6.1	7	6.1	0.38	0.13
44	6.1	7	6.1	0.38	0.13
45	5.32	1.96	5.32	0.33	0.08
46	6.5	7.42	6.5	0.45	0.24
47	6.18	7.18	6.18	0.4	0.15
48	6.5	7.48	6.5	0.47	0.26
49	6.5	7.5	6.5	0.47	0.27

Table 4.25 Organ dose data in group II

Case No.	Organ dose (mGy per series)				
	brain	**lens**	**salivary gland**	**skin**	**thyroid**
1	9.9	11	9.9	0.73	0.47
2	9.75	11	9.75	0.69	0.38
3	6.2	7.2	6.2	0.4	0.15
4	6.5	7.5	6.5	0.47	0.27
5	10	11	10	0.78	0.64
6	9.89	11	9.89	0.73	0.46
7	6.63	7.6	6.63	0.53	0.45
8	9.6	11	9.6	0.65	0.3
9	9.9	11	9.9	0.73	0.47
10	10	11	10	0.78	0.65
11	6.5	7.5	6.5	0.45	0.23

Table 4.25 Organ dose data in group II (cont.)

Case No.	Organ dose (mGy per series)				
	brain	lens	salivary gland	skin	thyroid
12	6.5	7.45	6.5	0.46	0.25
13	6.5	7.46	6.5	0.46	0.25
14	9.85	11	9.85	0.71	0.43
15	9.3	11	9.3	0.6	0.22
16	6.2	7.2	6.2	0.4	0.15
17	10	11	10	0.83	0.86
18	6.62	7.6	6.62	0.52	0.44
19	10	12	10	1.1	4.18
20	9.84	11	9.84	0.71	0.43
21	6.4	7.4	6.4	0.43	0.2
22	9.5	11	9.5	0.63	0.26
23	6.5	7.5	6.5	0.47	0.27
24	6.1	7	6.1	0.38	0.13
25	9.7	11	9.7	0.68	0.35
26	9.7	11	9.7	0.68	0.35
27	10	11	10	0.81	0.72
28	9.71	11	9.71	0.68	0.36
29	10	11	10	0.78	0.64
30	9.7	11	9.7	0.68	0.35
31	9.78	11	9.78	0.7	0.39
32	9.25	10.8	9.25	0.6	0.22

Table 4.25 Organ dose data in group II (cont.)

Case No.	Organ dose (mGy per series)				
	brain	lens	salivary gland	skin	thyroid
33	9.9	11	9.9	1.39	0.48
34	6.5	7.42	6.5	0.45	0.24
35	6.5	7.47	6.5	0.46	0.26
36	9.9	11	9.9	0.7	0.4
37	12	14	12	0.42	0.18
38	9.59	11	9.59	0.65	0.3
39	9.9	11	9.9	0.75	0.55
40	9.89	11	9.89	0.73	0.46

Table 4.26 Organ dose data in group III

Case No.	Organ dose (mGy per series)				
	brain	lens	salivary gland	skin	thyroid
1	15	16	15	0.97	0.58
2	15	16	15	0.99	0.65
3	15	16	15	1	0.67
4	9.9	11	9.9	0.73	0.47
5	15	16	15	0.97	0.59
6	16	16	16	1.1	1
7	16	16	16	1.11	1.02
8	10	11.4	10	0.84	1.03
9	15	16	15	0.97	0.58

Table 4.26 Organ dose data in group III (cont.)

Case No.	Organ dose (mGy per series)				
	brain	lens	salivary gland	skin	thyroid
10	15	16	15	0.97	0.58
11	16	16	16	1.1	1
12	9.7	11	9.7	0.68	0.35
13	6.5	7.43	6.5	0.46	0.24
14	16	16	16	1.1	1
15	15	16	15	0.98	0.61
16	15	16	15	0.99	0.64
17	15	16	15	0.99	0.62
18	16	17	16	1.2	1.42
19	15	16	15	0.98	0.6
20	15	16	15	0.97	0.59
21	16	16	16	1.1	1
22	9.73	11	9.73	0.69	0.36
23	15	16	15	0.97	0.59
24	16	17	16	1.3	1.8
25	14.63	15	14.63	0.86	0.37
26	15	16	15	0.99	0.63
27	16	16	16	1.18	1.16
28	16	16	16	1.13	1.05
29	15	16	15	0.97	0.58

Table 4.27 Organ dose data in group IV

Case No.	Organ dose (mGy per series)				
	brain	lens	salivary gland	skin	thyroid
1	18	19	18	1.2	0.7
2	19.55	20.55	19.55	1.63	2.57
3	13	13	13	0.9	0.83
4	10	11	10	0.67	0.45
5	18.64	19.64	18.64	1.26	0.87
6	19	20	19	1.3	1.13
7	18.59	19.59	18.59	1.26	0.86
8	19	20	19	1.3	1.2
9	19	20	19	1.5	2.2
10	18	19	18	1.2	0.7
11	19	20	19	1.3	1.1
12	18	19	18	2.3	0.7
13	19	20	19	1.3	1.2
14	18	19	18	2.3	0.7
15	17	18.93	17	1	0.45
16	18	19	18	2.3	0.75
17	19	20	19	1.33	1.25
18	18	19	18	1.1	0.61
19	15	16	15	0.98	0.61
20	15	16	15	0.98	0.6
21	18	20	18	2.3	0.75
22	18	19	18	1.2	0.7
23	18	22	18	2.3	0.76

Table 4.27 Organ dose data in group IV (cont.)

Case No.	Organ dose (mGy per series)				
	brain	lens	salivary gland	skin	thyroid
24	18	23	18	2.3	0.71
25	18.31	19.31	18.31	1.23	0.83
26	19	20	19	1.6	2.5
27	19	20	19	1.3	1.1

Table 4.28 Organ dose in each age group

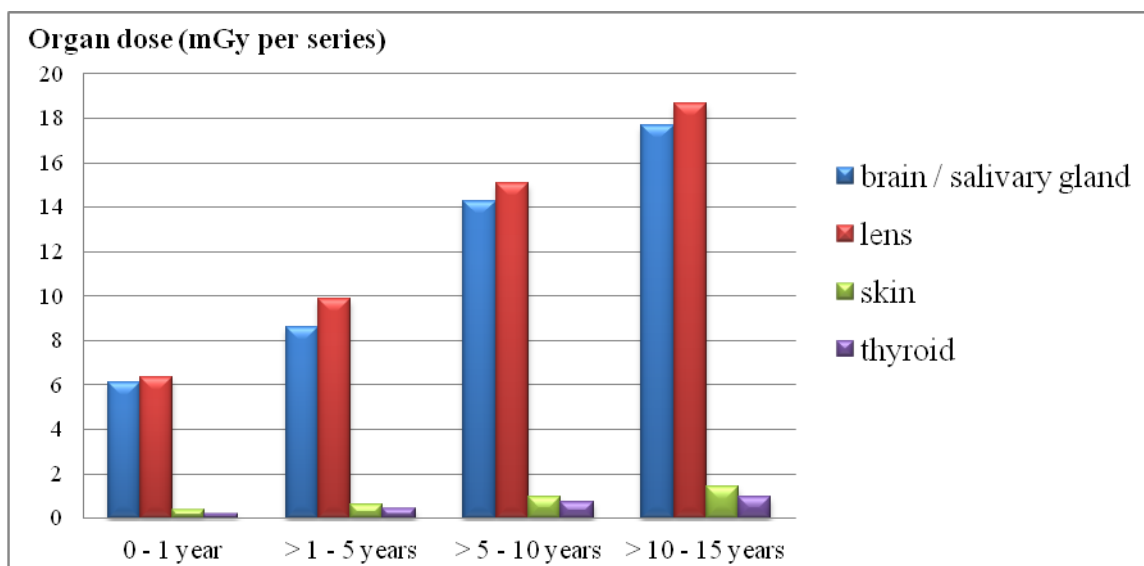| Group		Organ dose (mGy per series)				
		brain	lens	salivary gland	skin	thyroid
1	mean	6.13	6.36	6.13	0.41	0.19
	range	3.27 – 6.8	0.37 – 7.7	3.27 – 6.8	0.21 – 0.6	0.05 – 0.8
2	mean	8.61	9.85	8.61	0.65	0.47
	range	6.1 - 10	7 - 12	6.1 - 10	0.38 – 1.39	0.13 – 4.18
3	mean	14.29	15.06	14.29	0.97	0.75
	range	6.5 - 16	7.43 - 17	6.5 - 16	0.46 – 1.3	0.24 – 1.8
4	mean	17.67	18.67	17.67	1.46	0.99
	range	10 - 19.55	11 – 20.55	10 – 19.55	0.67 -2.3	0.45 – 2.57

Figure 4.7 Organ dose in each age group

Table 4.29 The average organ dose for deterministic risk estimation.

Group	Organ dose (mGy per series)				
	brain	lens	salivary gland	skin	thyroid
1	6.13	6.36	6.13	0.41	0.19
2	8.61	9.85	8.61	0.65	0.47
3	14.29	15.06	14.29	0.97	0.75
4	17.67	18.67	17.67	1.46	0.99

Table 4.30 Effective dose and stochastic risk to patient undergoing Head CT

Group	Effective dose (mSv per series)	Fatal cancer $5.0\ \%\ Sv^{-1}$	Non-fatal cancer $0.8\ \%\ Sv^{-1}$	Hereditary effect $1.3\ \%\ Sv^{-1}$	Total $7.3\ \%\ Sv^{-1}$
1	0.769	3.85×10^{-5}	6.15×10^{-6}	1.00×10^{-5}	5.62×10^{-5}
2	0.736	3.68×10^{-5}	5.88×10^{-6}	9.56×10^{-6}	5.37×10^{-5}
3	0.736	3.68×10^{-5}	5.88×10^{-6}	9.56×10^{-6}	5.37×10^{-5}
4	0.764	3.83×10^{-5}	6.13×10^{-6}	9.96×10^{-6}	5.59×10^{-5}

CHAPTER V

DISCUSSION AND CONCLUSION

5.1 Discussion

Quality control of the CT system is very important and should be firstly performed. The CT Dose was measured following IAEA Human Health series No.19. The pencil ionization chamber, 100 mm length was used to measure the computed tomography dose index (CTDI) in air and in phantoms to obtain weighted computed tomography dose index ($CTDI_w$) values for head and body protocols in all kVp.

The $CTDI_{100}$ in air increased from 80 kVp to 140 kVp in head and body protocols. When compare the measurements with ImPACTSCAN, 0.67 and 2.81 in head protocol, 0.47 and 2.68 in body protocol, the measurements were lower than the ImPACTSCAN of less than 10%.The measurement values agree with ImPACTSCAN values.

The calculated $CTDI_w$ was higher than the displayed $CTDI_{vol}$ values in all kVp settings for head and body protocols but lower than ImPACT except at 80 kVp. The percentage differences of calculated $CTDI_w$ values and ImPACT in head were less than 10%, -5.76 to 7.45. But the displayed $CTDI_{vol}$ and ImPACT values are at large difference of 19 - 34% and the correction factors should be provided. For body protocol, the percentage differences of calculated $CTDI_w$ values with ImPACT values were less than 10% (-5.39 – 3.76). In this study, the protocol for pediatric patients is small FOV similar to head protocol. The correction factor for body protocol is not required to apply in this study.

From the IAEA Technical Report Series (TRS) No.457: Dosimetry in Diagnostic Radiology: An International Code of Practice [21], the discrepancy between the measurement and the displayed values came from the measurement uncertainty. The factors affecting the measurement uncertainty to estimate the CTDI were the characteristics of ionization chamber and electrometer, the measurement scenario, the precision of reading, tube loading, chamber positioning, the phantom construction, the chamber response in phantoms and the inaccuracy on laser beam alignment.

145 pediatric patients were scanned according to particularly protocol and depending on age. The patient data, scanning parameters and radiation dose were recorded from the data on PACs system. The patient information consist of 79 boys and 66 girls, mean ages were 5.3 months, 2.7, 7.6 and 12.3 years in age group 1 to 4, respectively.

For group I and II, 100 kVp was selected and group III and IV 120 kVp was selected. Lowest mA at 100 was set for group I, 150 for group II and III and highest set at 180 for group IV. The same rotation time 0.5 second was set for all groups, collimation 20 mm, slice thickness 5 mm and pitch 0.969:1. Mean scan length of group 1 to 4 were 122.3, 140.7, 144.3 and 145.0 mm, respectively.

Mean (range) of CTDI$_{vol}$ per series increase from 7.15 (3.7 – 7.6), 9.68 (6.4 – 11.4), 15.59 (10.2 – 17.3) to 19.45 (11.5 – 20.7) mGy from age group I to IV, respectively. Mean (range) of DLP per series increase from 69.93 (30.0 – 92.5), 109.79 (66.1 – 165.1), 183.93 (99.1 – 271.9) to 239.42 (149.2 – 338.0) mGy.cm from age group I to IV respectively. Effective radiation dose was estimated from the DLP multiplied a conversion coefficient for age group I to IV of 0.011, 0.0067, 0.0040 and 0.0032 mSv/mGy.cm. The mean effective dose per series in Group IV was 0.764 mSv and highest in Group I of 0.769 mSv, Group II and III equal to 0.736 mSv.

Group I, case no.18, same parameters setting except scan length at pre contrast of 145 mm, post contrast 135 mm, CTDI$_{vol}$ was the same of 5.68 mGy but DLP first was 95.3 mGy.cm and last 89.7 mGy.cm. Case no. 44 the tube current first was 50 mA and last 55 mA resulted in increased CTDI$_{vol}$ from 5.18 to 5.7 mGy and DLP from 70.6 to77.7 mGy.cm.

Group II, case no.1, same parameters setting except scan type was helical and then axial mode and slightly different in scan length of 145 and 136.9 mm respectively. Both CTDI$_{vol}$ and DLP decreased, first were 8.5 mGy, 143 mGy.cm and last 8.1 mGy, 115.4 mGy.cm. Case no. 3 different in scan length pre contrast 120 mm, post contrast 125 mm, the same CTDI$_{vol}$ at 5.68 mGy but DLP first was 81.1 mGy.cm and last 84.0 mGy.cm.

Group III, case no.26, same parameters setting except scan type was axial and then helical mode, and slightly different in scan length 137.5 and 130 mm, respectively. Both CTDIvol and DLP increased, first was 13.3 mGy, 186.4 mGy.cm and last 13.8 mGy, 210 mGy.cm.

Group IV, case no.2, radiation dose increases from several the factors, different in scan type, tube current and scan length. Both CTDI$_{vol}$ and DLP increased, from 15.4 to 16.7 mGy and 287.6 to 388.3 mGy.cm respectively.

In this study, factors affecting radiation dose to pediatric patients were scan type, scan length, tube current and number of series. There were variations in the scanning techniques in larger children by inappropriately selecting adult protocols for large children and by making mistakes in the cut-off ages for pediatric CT

Head CT scan by 64 slices CT at Imaging Center Siriraj Hospital, when patients were scanned at two series, without and with contrast, resulting in the double CTDI$_{vol}$ (mGy), DLP (mGy.cm) and effective dose (mSv) as shown in table 5.1.

Table 5.1 Mean radiation dose data compare 1 and 2 series in all age group.

AGE	CTDI$_{vol}$ (mGy)		DLP (mGy.cm)		Effective dose (mSv)	
	1 series	2 series	1 series	2 series	1 series	2 series
0-1 yr	7.05	15.04	70.92	144.04	0.78	1.58
1 - 5 yr	9.59	19.58	108.07	223.38	0.72	1.50
6 - 10 yr	16.03	29.66	190.90	341.34	0.76	1.37
11 - 15 yr	19.97	37.75	238.03	479.64	0.76	1.53

In pediatric patients with abnormalities in the temporal, PNS, and orbits, the helical mode was selected for smooth reconstruction and the movement of patients was reduced for the shorter scan time using the helical mode, the scan time in axial is longer. If the axial mode was selected, the scan may be repeated, properly protocol selection is also another good parameter for dose reduction.

Table 5.2 Mean radiation dose data between axial and helical modes in all age group.

AGE(yr)	CTDI$_{vol}$ (mGy)		DLP (mGy.cm)		Effective dose (mSv)	
	axial	helical	axial	helical	axial	helical
0-1	7.29	7.56	69.47	84.19	0.76	0.93
1 - 5	9.61	10.02	106.96	119.27	0.72	0.80
6 - 10	15.52	17.29	180.36	240.95	0.72	0.96
11 - 15	19.15	20.77	225.57	306.36	0.72	0.98

This study was the first pediatric head CT dose collection at Siriraj Hospital. Comparison with other three university hospitals with large volume of pediatric CT studies with various types of scanners **[13]**, the CTDI and DLP in this study were less than other three hospitals in all age groups. One of the reasons for this difference might be CT parameter settings among the different scanners.

Table 5.3 Mean radiation dose compare with other University hospitals in Thailand in all age group.

AGE	CTDI$_{vol}$* (mGy)				DLP (mGy.cm)			
	This study	Center A**	Center B***	Center C****	This study	Center A**	Center B***	Center C****
0-1 yr	7.0	24.3	13.6	26.7	70.9	292	194	472
1 - 5 yr	9.6	30.3	16.2	26.8	108.1	429	270	542
6 - 10 yr	16.0	39.0	20.4	35.1	190.9	702	372	625
11 - 15 yr	20.0	62.0	26.8	35.7	238.0	742	487	763

*   CTDI$_{vol}$ used in Centers B and C, CTDI$_w$ used in Center A

**   **Siemens**; Somatom Sensation 4 MSCT and Somatom Sensation 16

***   **Siemens**; Somatom Definition

**** **Philips**; Brillance 64

In comparison to other studies [14], [17] with similar acquisition protocol, the effective dose in this study is smaller than DRLs in UK2003, EU and the others because of the lower setting parameters. Fujii K., el al [14] studied organ doses in infant CT examinations with multi-detector row CT scanners. Radiation doses were measured with radiophotoluminescence glass dosemeters set at skin over various organ positions within a 1-y-old child anthropomorphic phantom and organ doses were evaluated from the measurement values. Doses for tissues or organs within the scan range were 28–36 mGy in an infant head CT. Organ dose at brain, lens, salivary gland, skin and thyroid were 31.9, 35.8, 12.3, 3.8 and 1.2 mGy respectively which were higher than this study of 6.1, 6.4, 6.1, 0.4 and 0.2 mGy respectively. Mazonakis M., et al [17] studied thyroid dose and the associated risk for thyroid cancer induction from common head and neck computed tomography (CT) examinations during childhood. The Monte Carlo N-particle transport code was employed to simulate the routine CT scanning of the brain, paranasal sinuses, inner ear and neck performed on axial and/or helical modes. The mean thyroid dose was calculated using mathematical phantoms representing a newborn infant and children of 1, 5, 10 and 15 years old. The scattered dose to thyroid from head CT examinations varied from 0.6 to 8.7 mGy depending upon the scanned region, the pediatric patient's age and the acquisition mode used. The thyroid dose received from brain, sequential protocol based on age group I-IV were 2.3, 2.8, 2.1 and 2.2 mGy respectively which were higher than this study of 0.19, 0.47, 0.75 and 0.99 mGy.

Reviews of biological and clinical studies have shown that the amount of radiation producing the deterministic effects was below 0.5 Gy for cataract occurrence. Deterministic effects are associated with a threshold dose, will only occur if the most highly irradiated tissue exceeds the threshold dose and above which the risks become more likely to occur with increasing dose. In addition, deterministic effect severity often increases with increasing dose. This is primarily due to the fact that cellular repair mechanisms occur continuously and this prevents deterministic effects at low radiation exposure levels. The effects from radiation exposures at X-ray energies do not occur during or immediately after the exposure to radiation, shown in the Table 5.4 in column labeled "Time to develop effect". The effects from these high-absorbed radiation doses require weeks to years following the exposure to produce the effects. Therefore, the effect will not be seen at the time of exposure and when the effect does occur the correlation to the radiation exposure may not be easily determined [22]. Although deterministic effects have occurred in high-dose procedures, such as perfusion CT imaging, they are expected to be rare when examinations are performed by individuals who are well trained in medical imaging and radiation dosimetry.

Table 5.4 Dose Threshold for Deterministic Effects **[23]**

Tissue	Total acute dose threshold (Gy)	Time to develop effect
Brain*		
Necrosis	NA	> 1 year
Cognitive defects	1 – 2	several years
Cognitive defects infants < 18 months	0.1 – 0.2	several years
Lens of eye**		
Detectable opacities	0.5 – 2	> 1 year
Cataract formation	0.5	> 1 year
Salivary glands*		
Xerostomia	NA	1 week
Skin**		
Skin reddening	3 – 6	1 – 4 weeks
Temporary hair loss	4	2 – 3 weeks
Skin death and scarring	5 – 10	1 – 4 weeks
Thyroid*		
Endocrine dysfunction	NA	> 10 years

* ICRP publication 118 Ann. ICRP 41(1/2).
** www.imagewisely.org

Organ dose were determined by **ImPACT CT Patient Dosimetry Calculator Version 1.0.4** according to ICRP 103 in brain, lens, salivary glands, skin and thyroid. In this study organ dose in one series was less than 0.02 Gy as shown in Table 5.5 result that all of them are less than the effect of cataract. Accordingly, deterministic effects of cataract would not be occurred for any pediatric patient undergoing head CT examination at Imaging Center, Siriraj Hospital.

Table 5.5 The average organ dose determined by ImPACTSCAN software.

Group	Organ dose (mGy per series)				
	brain	lens	salivary gland	skin	thyroid
1	6.13	6.36	6.13	0.41	0.19
2	8.61	9.85	8.61	0.65	0.47
3	14.29	15.06	14.29	0.97	0.75
4	17.67	18.67	17.67	1.46	0.99

Stochastic effects are carcinogenesis and genetic effects. The principal concern for any patient undergoing CT examination is the risk of developing a radiation-induced cancer, which may be fatal or nonfatal [24]. The total patient risk is related to the effective dose is measured in sieverts (Sv) as shown in Table 5.6 which depends on the dose to patient age, as well as its radiosensitivity. At the low doses associated with diagnostic radiologic examinations, the radiation risk is generally taken to be proportional to the cumulative organ dose. The radiation risk from two CT scans would be approximately twice the risk of a single scan, irrespective of the time interval between the two CT scans.

In standard head CT protocol for pediatric patient in each age group, the effective dose in each group were 0.769, 0.736, 0.736 and 0.764 mSv corresponds to a total radiation risk of approximately 5.61, 5.37, 5.37 and 5.58 per 100,000 individuals undergoing head CT examination. Highest risk in fatal cancer are 3.85, 3.68, 3.68 and 3.82 radiation-induced cancers per 100,000 individuals undergoing head CT examination. Lowest risk in non-fatal cancer was 6.15, 5.88, 5.88 and 6.13 per 1,000,000 individuals undergoing head CT examination.

Table 5.6 Effective dose and stochastic risk to patient undergoing Head CT examination.

Group	Effective dose (mSv per series)	Fatal cancer 5.0 % Sv^{-1}	Non-fatal cancer 0.8 % Sv^{-1}	Hereditary effect 1.3 % Sv^{-1}	Total 7.3 % Sv^{-1}
1	0.769	3.85×10^{-5}	6.15×10^{-6}	1.00×10^{-5}	5.62×10^{-5}
2	0.736	3.68×10^{-5}	5.88×10^{-6}	9.56×10^{-6}	5.37×10^{-5}
3	0.736	3.68×10^{-5}	5.88×10^{-6}	9.56×10^{-6}	5.37×10^{-5}
4	0.764	3.83×10^{-5}	6.13×10^{-6}	9.96×10^{-6}	5.59×10^{-5}

Routine protocols for pediatric head CT acquires adequate image quality for giving essential information in case of emergency such as skull fracture, intracerebral hemorrhage or large area of infarction or brain herniation or degree of brain edema or hydrocephalus. Abnormal calcification in side brain mass or gross abnormal enhancing mass or abnormal vascular condition such as dural venous sinus thrombosis or arteriovenous malformations can be primary evaluation before further specific investigation. Images from slice thickness 5 mm probably show better quality than 1.25 mm slice thickness. Figure 5.1 shown CT image from different age group, group 1 *(0-1yr)* probably be the most difficult to interpret but still maintain essential preliminary information for diagnosis in case of emergency condition. Other groups showed satisfactory quality. It is important to reduce radiation dose but still achieve quality diagnostic images which is essential to obtain an accurate and reliable diagnosis. Established appropriate protocol following clinical indication to prevent excess doses such as in the case of hydrocephalus which follow up shunt can reduce exposure and scan length. However radiation dose in this study report that $CTDI_{vol}$ and DLP were still much below the DRL recommendations from UK2003 and EU. Furtheremore slightly adjust the exposure parameters can improve image quality provide better.
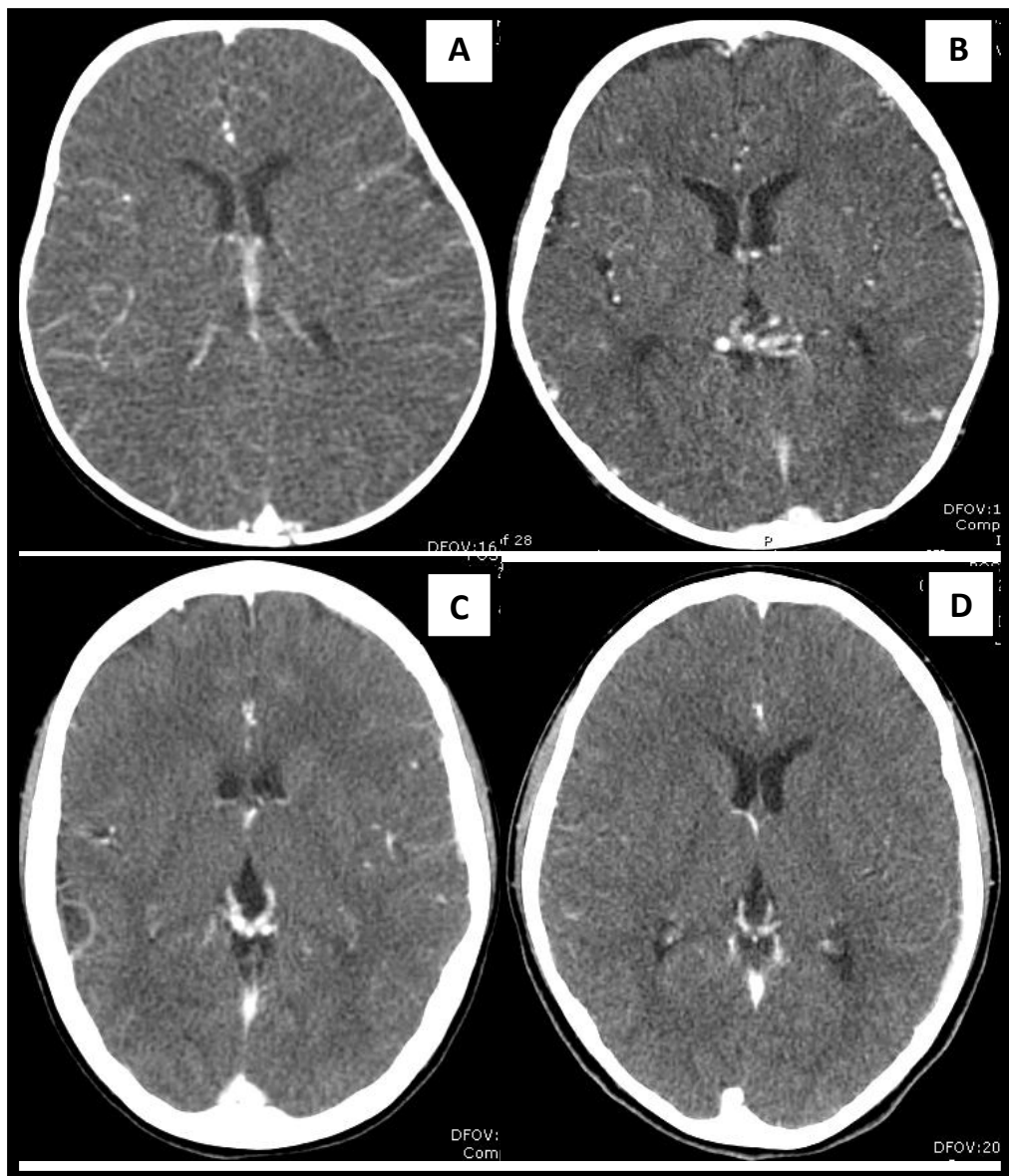
Figure 5.1 CT images in different age group
(**A**) '0-1 yr', (**B**) '>1-5 yrs', (**C**) '>5-10 yrs' and (**D**) '>10-15 yrs'.

5.2 Conclusion

CTDI measurements provide the data to verify radiation dose display on monitor at work station. The calculated CTDI and DLP values and the monitor value were different at higher than ± 5% percent. Therefore, the CTDI and DLP values shown on PACs system will be applied with correction factors to obtain the most correct patient dose.

From this study, the dose reference level, third quartile values for head CT examination had been compared with recommendations from the Switzerland, Germany, UK2003 and EU national reference doses for pediatric patients from various age groups as shown in Table 5.7.

Table 5.7 DRLs (mGy for CTDI and mGy.cm for DLP) for different patient groups and examinations and in this research, Switzerland, Germany, UK2003, and EU.

Age Group	Quantity	This study	Switzerland	Germany	UK 2003	EU
< 1 year	CTDI$_{vol}$	7	20	33	30	
	DLP	77	270	390	270	300
1-5 years	CTDI$_{vol}$	11	30	40	45	
	DLP	130	420	520	470	600
5-10 years	CTDI$_{vol}$	17	40	50	50	
	DLP	213	560	710	620	750
10-15 years	CTDI$_{vol}$	20	60	60	65	
	DLP	256	1000	920	930	

Risks associated with lower levels of radiation are periodically reviewed by leading scientific organizations, including the ICRP**,** the US National Academy of Sciences Committee on the Biological Effects of Ionizing Radiation (BEIR), and the UN Scientific Committee on the Effects of Atomic Radiation (UNSCEAR)**.** For practical radiation protection purposes, these scientific bodies recommend that the carcinogenic radiation risk is taken to be directly proportional to the absorbed radiation dose, with no threshold dose**.**

The risk and benefit from medical exposures are received by the same individual. Since the individual's situation, body habitus, and medical needs are unique, dose limits are not used for medical exposures. An average radiation exposure level received from a diagnostic or interventional procedure can be used to evaluate whether the dose being used for a procedure is within an acceptable range. With an understanding of the effects of radiation and the doses for standard examinations, a physician and a radiologist can make a determination of which examination provides the most benefit to the patient at the lowest possible dose.

This study described a method for estimating radiation doses and the corresponding radiation risks for pediatric patients based on organ dose from The ImPACT CT Patient Dosimetry Calculator and effective dose.

The result of this study leads to the organ doses in the scan area undergoing head CT examination and radiation risk in critical organs of pediatric patient. Patient doses and biological effects in CT need to be weighed against the anticipated patient benefits from the diagnostic information obtained. In addition, it is also important to ensure that patient doses are kept as low as reasonably achievable and the patient risks are minimized. Although the balance of risks and benefits are still strongly towards benefit, there is the requirement for precaution. As the frequency of pediatric CT examinations is rapidly increasing, the radiation risks for children undergoing CT are not negligible. More active reduction of CT exposure settings should play an important role in pediatric patients.

REFERENCES

[1]   Strauss KJ, et al. Image gently: Ten steps you can take to optimize image quality and lower CT dose for pediatric patients. **American journal of roentgenology** 194, 4 (2010) : 868-873.

[2]   Vock P. CT dose reduction in children. **European radiology** 15, 11 (2005) : 2330-2340.

[3]   Shrimpton PC, Hillier MC, Lewis MA, Dunn M. National survey of doses from CT in the UK: 2003. **The British journal of radiology** 79, 948 (2006) : 968-980.

[4]   **Wikipedia the Free Encyclopedia** [Online]. 2012. Available from : http://en. wikipedia.org/wiki/X-ray_computed_tomography [2012, August 19].

[5]   ICRP- International Commission on Radiological Protection. Managing patient dose in multi-detector computed tomography (MDCT), **ICRP Publication 102 Annals of the ICRP** 37, 1(2007) : 1-79.

[6]   Jessen KA, Panzer W, Shrimpton PC, et al. **EUR 16262: European Guidelines on Quality Criteria for Computed Tomography.** Luxembourg: Office for Official Publications of the European Communities, 2000.

[7]   Jones DG, Shrimpton PC. **Survey of CT Practice in the UK. Part 3: Normalised Organ Doses Calculated Using Monte Carlo techniques**. Oxon: National Radiological Protection Board, 1991.

[8]   ICRP- International Commission on Radiological Protection. Recommendations of the International Commission on Radiological Protection. **ICRP Publication 60 Annals of the ICRP** 21 (1991) : 1-3.

[9]   ICRP- International Commission on Radiological Protection. Diagnostic reference levels in medical imaging: review and additional advice. **Annals of the ICRP** 31, 4 (2001) : 33-52.

[10]   Frush DP, Applegate K. Computed tomography and radiation: understanding the issues. **Journal of the American College of Radiology** 1 (2004) : 113-119.

[11]   Boone JM, Geraghty EM, Seibert JA, Wootton-Gorges SL. Dose reduction in pediatric CT: a rational approach. **Radiology** 228 2 (2003) : 352-360.

[12]   Callahan MJ. CT dose reduction in practice. **Pediatric radiology** 41 (2011) : 488-492.

[13]   Kritsaneepaiboon S, Trinavarat P, Visrutaratna P, et al. Survey of pediatric MDCT radiation dose from university hospitals in Thailand: a preliminary for national dose survey. **Acta Radiologica** 53 (2012) : 820–826

[14] Fujii K, Akahane K, Miyazaki O, Horiuchi T, Shimada A, Nagmatsu H, et al.
      Evaluation of organ doses in CT examinations with an infant
      anthropomorphic phantom. **Radiation protection dosimetry** 147, 1-2
      (2011) : 151-155.

[15] Huda W. Radiation doses and risks in chest computed tomography
      examinations**. Proceedings of the American Thoracic Society** 4, 4
      (2007) : 316-320.

[16] Huda W, Ogden KM, Khorasani MR. Converting dose-length product to
      effective dose at CT. **Radiology** 248, 3(2008) : 995-1003.

[17] Mazonakis M, Tzedakis A, Damilakis J, Gourtsoyiannis N. Thyroid dose
      from   common head and neck CT examinations in children: is
      there an excess risk for thyroid cancer induction?. **European
      radiology** 17, 5 (2007) : 1352-1357.

[18] Li X, Samei E, Segars WP, Sturgeon GM, Colsher JG, Frush DP. Patient-
      specific radiation dose and cancer risk for pediatric chest CT.
      Radiology 259, 3 (2011) : 862-874.

[19] International Atomic Energy Agency. **HUMAN HEALTH SERIES No. 19:
      Quality Assuarance Programme for Computed Tomography
      Diagnostic and Therapy Applications.** Vienna, 2012.

[20] ImPACT. **ImPACT information leaflet 1: CT scanner acceptance testing**.
      Version 1.02, (2001) : 1-8.

[21] International Atomic Energy Agency. **Dosimetry in Diagnostic Radiology :
      An International Code of Practice.** Technical report series no. 457.
      Vienna: International Atomic Agency, 2007.

[22] Donald J. Peck, Ehsan Samei. **How to Understand and Communicate
      Radiation Risk** [Online]. 2010. Available from :
      http://www.imagewisely.org/Imaging-Professionals/Medical-
      Physicists/Articles/How-toUnderstand-and-Communicate-Radiation-
      Risk [2012, September 22]

[23] ICRP- International Commission on Radiological Protection. Draft report
      for consultation, Early and late effects of radiation in normal
      tissues and organs: threshold doses for tissue reactions and other
      non-cancer effects of radiation in a radiation protection context.
      Annals of the ICRP 41 (2011) : 269-286.

[24] Brenner D, Elliston C, Hall E, Berdon W. Estimated risks of radiation-
      induced fatal cancer from pediatric CT. **American journal of
      roentgenology** 176, 2 (2001) : 289-296.

APPENDICES

Appendix A Case Record Form

Table 1 Data Collection form of patient information

Date of CT scan   _____

☐ The office hours   ☐ Outside office hours

Sex _____   **Age** _____   **Weight** _____ **kg**

Diagnosis   _____

Sedation   ☐   Yes   ☐   No

Type of CT exam   _____

Series 1   **Scout** ☐ **AP** ☐ **PA**   ☐ **Lat**

Series 2   _____

Series 3   _____

Series 4   _____

Series 5   _____

Phase	Scan type	kVp	mA	t_{rot}	Pitch	Thickness	Scan length		CTDI$_{vol}$	DLP
							upper	lower		

Appendix B Quality Control of CT system

1. Scan Localization Light Accuracy

Purpose: To test congruency of scan localization light and scan plane.

Method: Tape Localization film to the backing plate making sure that the edges of the film are parallel to the plate edge. Place the film vertically along the midline of the couch aligned with its longitudinal axis. Raise the table to the head position. Turn the alignment light. Mark both internal and external light with unique pin pricks along the midline of the light. Expose the internal light localization using the narrowest slice setting at 120-140 kVp, 50-100 mAs. For external light increment table to light position under software control and expose the film.

Tolerance: The center of the irradiation field should be less than 2 mm.

Result: Pass

Measured Deviation	External	0	mm
	Internal	1.24	mm

Comments: Accuracy of external light systems depends on both table incrementation accuracy and light alignment, since they are designed to indicate a plane a specific distance from the scan plane.

2. Alignment of Table to Gantry

Purpose: To ensure that long axis of the table is horizontally aligned with a vertical line passing through the rotational axis of the scanner.

Method: Locate the table midline using a ruler and mark it on a tape affixed to the table. With the gantry untilted, extend the table top into gantry to tape position. Measure the horizontal deviation between the gantry aperture centre and the table midline.

Tolerance: The deviation should be within 5 mm .

Result: Pass

	Table	Bore
Distance from Right to Center (mm)	210	351
Distance from Centre to Left (mm)	210	349
Measured Deviation (mm)*	**0**	**1**

*Measured deviation = (Distance from right to center – Distance from center to left)/2

Comments: Misalignment can cause image artifacts with large patients if patient extends out of the sampled area

3. Table Increment Accuracy

Purpose: To determine accuracy and reproducibility of table longitudinal motion.

Method: Tape a measuring tape at the foot end of the table. Place a paper clip at the center of the tape to function as an indicator. Load the table uniformly with 150 lbs. From the initial position move the table 300, 400 and 500 mm into the gantry under software control. Record the relative displacement of the pointer on the ruler. Reverse the direction of motion and repeat. Repeat the measurements four times.

Tolerance: Positional errors should be less than 3 mm at 300 mm position.

Indicated (mm)	Measured (mm)	Deviation (mm)
500	500	0
400	400	0
300	300	0
- 300	- 300	0
- 400	- 401	1
- 500	- 501	1

Deviation = | Indicated – Measured|

Comments: Under computer control from operators console the patient table must be able to accurately and reproducibly move the patient to any indicated position in the scan field. Accuracy is critical since it determines relative locations of image sections and influences the multi-scan dose.

4. Slice Increment Accuracy

Purpose: To Determine the accuracy of the slice increment.

Method: Set up as you would for beam profile measurement. Select 120 kVp, 100 mAs, and smallest slit width. Perform several scans with different programmed slice separations under auto control. Scan the film with a densitometer and measure the distance between the peaks.

Tolerance: Position errors should be less than 3 mm at 300 mm position.

Result: Pass

Slice Separation in mm	Measured Separation in mm	Deviation (mm)
20	19.07	0.93
30	30.48	0.48
50	48.93	1.07

Deviation = |Slice separation – Measured separation|

Comments: Under computer control from operators console the patient table must be able to accurately and reproducibly move the patient to any indicated position in the scan field. Accuracy is critical since it determines relative locations of image sections and influences the multi-scan dose.

5. Gantry Angle Tilt

Purpose: To determine the limit of gantry tilt and the accuracy of tilt angle indicator.

Method: Tape a localization film to the backing plate making sure that the edges of the film are parallel to the edges of the backing plate. Place the film vertically along the midline of the couch aligned with its longitudinal axis. Raise the table to the head position. Move the table into the gantry. Center plate to alignment light. Expose the film at inner light location using narrowest slit, 120-140 kVp, 50-100 mAs. Tilt the gantry to one extreme from the console. Record the indicated gantry angle. Expose the film using the above technique. Measure the clearance from the closest point of gantry to midline of the table.Tilt the gantry to its extreme in the opposite direction. Record clearance and repeat the exposure. Measure the tilt angles from the images on the film.

Tolerance: Deviation between indicated and measured tilt angles $\leq$ 3º. Gantry clearance should be $\geq$30 cm.

Result: Pass

	Away	Toward
Indicated Angle	30º	30º
Measured Angle	29.65º	29.77º
Deviation*	0.35	0.23
Clearence	30.2	37

Deviation = |Indicated angle – Measured angle|

Comments: Tilt indicators on gantry or table may not correspond to actual tilt or to that indicated on computer display. Some scanners may collide with the patient at extremes of tilt under some clinical conditions. Most scanners accomplish nonorthogonal scan planes by tilting the gantry, but some angle the table. Most table-tilting systems angle the table relative to the horizontal plane; however, pivoting of the table relative to the vertical plane is also seen.

6. Position Dependence of CT Numbers

Method: Position the water phantom centered in the gantry. Using 1 cm slice thickness, obtain one scan using typical head technique. Select a circular region of interest of approximately 400 sq. mm. and then record the mean C.T. number and standard deviation for each of the positions 1 through 5.

Technique: 120 kVp, 100 mA, 1 sec, 250 mm SFOV.

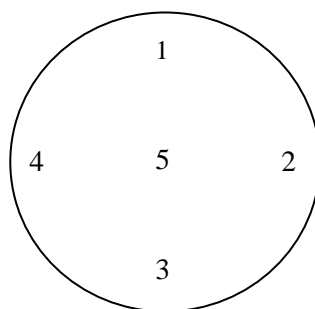**Tolerance:** The coefficient of variation of mean CT numbers of the four scans should be less than 0.2.

Figure I Position of ROI for CT number measurement.

Result:

Position	Mean C.T. #	S.D.	C.V.
1	114.78	6.67	0.058
2	112.68	12.01	0.107
3	113.35	12.26	0.108
4	113.60	9.88	0.087
5	117.76	11.43	0.097

CV = Standard deviation/mean CT number

Comments: Pass

7. Reproducibility of CT Numbers.

Method: Using the same set up and technique as position dependence, obtain three scans. Using the same ROI as position dependence in location 5, this is the center of the phantom obtain mean C.T. numbers for each of the four scans.

Tolerance: The coefficient of variation of mean CT numbers of the four scans should be less than 0.002.

Result: Pass

Run Number	1	2	3	4
Mean CT Number (HU)	117.63	117.63	117.51	117.73

Mean Global C.T. Number	117.625
Standard Deviation	0.090
Coefficient Of variation	0.001

8. mAs Linearity

Method: Set up the same as position dependence and insert 10 cm long pencil chamber in the center slot of the C.T. dose head phantom. Select the same kvp and time as used for head scan. Obtain four scans in each of the mA stations normally used in the clinic. For each mA station record the exposure in mGy for each scan. Scans should be performed in the increasing order of mA. Compute mGy/mAs for each mA setting.

Technique: 120 kVp, 100 mA, 1 sec, 250 mm SFOV

Result: Pass

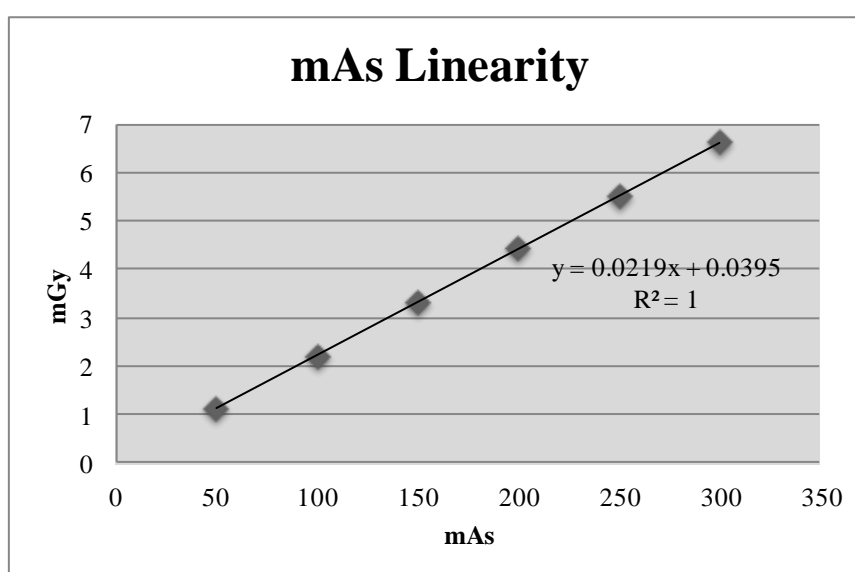| mA	Exposure in mGy				mGy/mAs	C.V.
	Run 1	Run 2	Run 3	Run 4		
50	1.131	1.13	1.127	1.129	0.02	1.000
100	2.238	2.238	2.234	2.234	0.02	0.005
150	3.348	3.335	3.34	3.332	0.02	0.002
200	4.444	4.428	4.44	4.433	0.02	0.002
250	5.515	5.526	5.522	5.515	0.02	0.002
300	6.619	6.604	6.626	6.634	0.02	0.000

Figure II The relationship of mGy and mAs

9. Linearity of CT Numbers

Method: Set up the catphan phantom as described in beam alignment. Select the section containing the test objects of different CT numbers. Select the head technique and perform a single transverse scan. Select a region of interest (ROI) of sufficient size to cover the test objects. Place the ROI in the middle of each test object and record the mean CT number.

Technique: 120 kVp, 300 mA, 1 sec, 180mm SFO, slice collimation 8 mm.

Tolerance: R-square between measured CT number and linear attenuation coefficient (μ) more than 0.9

Results: Pass

Material	Expected CT no. (HU)	Measured CT no. (HU)	$\mu(cm^{-1})$
Air (superior)	-1000	-1005.39	0
Polystyrene	-35	-39.5	0.162
LDPE	-100	-98.37	0.151
PMP	-200	-188.12	0.136
Air (inferior)	-1000	-1007.59	0
Teflon	990	999.67	0.305
Delrin	340	364.71	0.217
Acrylic	120	122.25	0.184

Note: Expected CT numbers are either the predicted ones or the ones obtained during the previous annual measurement.
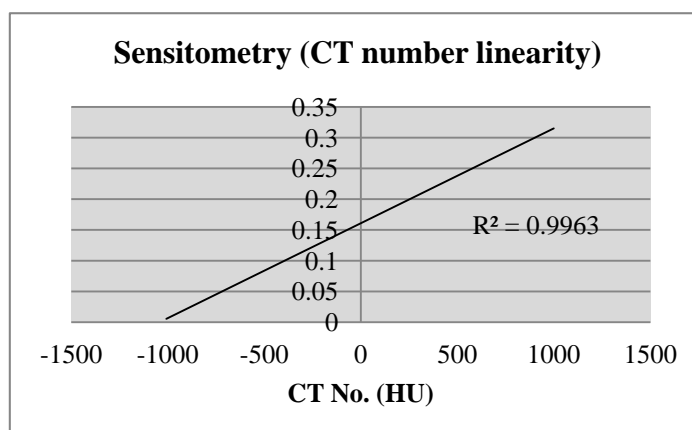
Comments:

Figure III Linearity of CT number

10. Accuracy of Distance Measurement

Purpose: To test accuracy of Distance Measurement and for circular symmetry of the CT image

Method: Set up the catphan phantom as described in beam alignment. Select the section containing the test accuracy of distance measurement. Select the head technique and perform a single transverse scan. Measured object in x and y axes.
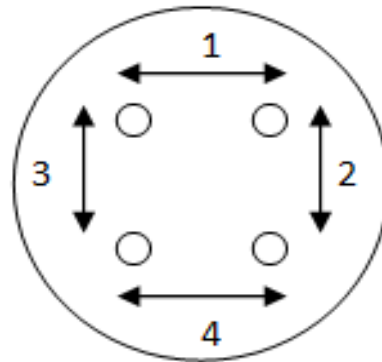
Figure IV Measuring directions.

Results:

Position	Indicate (mm)	Measured (mm)	Different (mm)
1	50	50	0
2	50	49.9	0.1
3	50	49.9	0.1
4	50	49.9	0.1

Comment: Pass

11. Image uniformity

Method: Set up the catphan phantom as described in beam alignment. Select the section containing the image uniformity module. Select the head technique. Perform a single transverse scan. Measure the mean value and the corresponding standard deviations in CT numbers within a region of interest (ROI). These measurements are taken from different locations within the scan field.

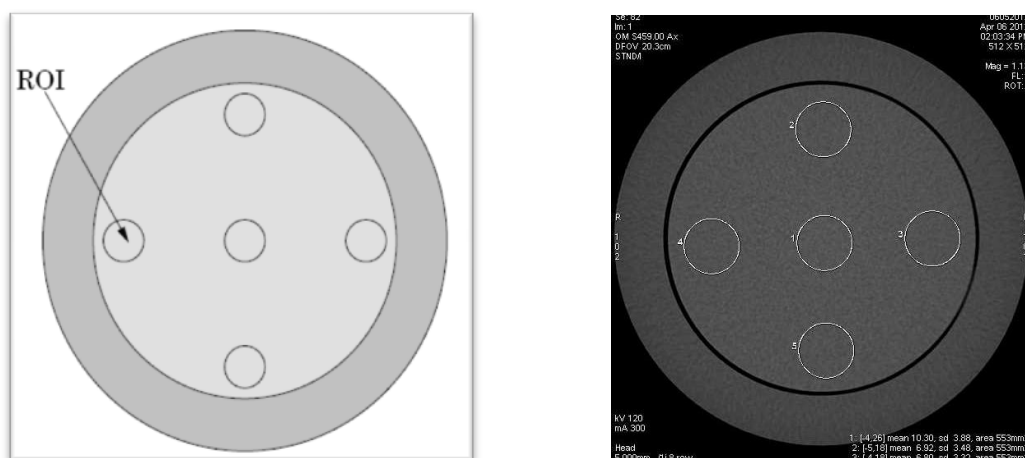**Technique:** 120 kVp, 300 mA, 1.0 sec, 250 mm SFOV

Tolerance: 5 HU

Results: Pass

Position	CT number (HU)	SD	Different (HU)
Center	10.92	3.88	0
3 o'clock	6.80	3.48	4.12
6 o'clock	6.90	3.44	4.02
9 o'clock	6.85	3.51	4.07
12 o'clock	6.92	3.32	4.00

Different = |CT number center – CT number peripheral|

Comment:

. **Figure V** Position of ROI for Image Uniformity measurement.

12. High Contrast Resolution

Method: Set up the catphan phantom as described in beam alignment. Select the section containing the high resolution test objects. Select the head technique. Perform a single transverse scan. Select the area containing the high resolution test objects and zoom as necessary. Select appropriate window and level for the best visualization of the test objects. Record the smallest test object visualized on the film.
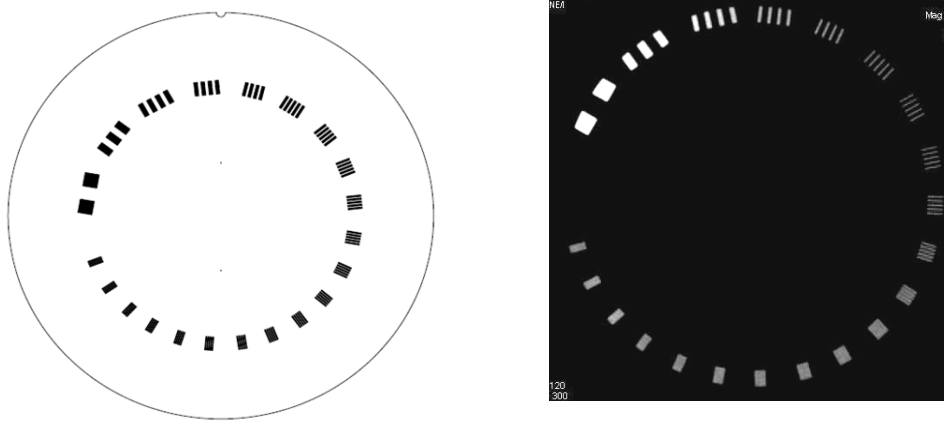
Technique: 120 kVp, 300 mA, 1.0 sec, 250 mm FOV

Figure VI High contrast resolution module

Result: Pass

Slice Thickness in mm	Resolution
1.25	12 lp/cm (0.042 mm)

13. Low Contrast Detectability

Method: Select the section containing the low resolution test objects in the mini phantom. Perform a single transverse scan utilizing the same technique as high resolution.

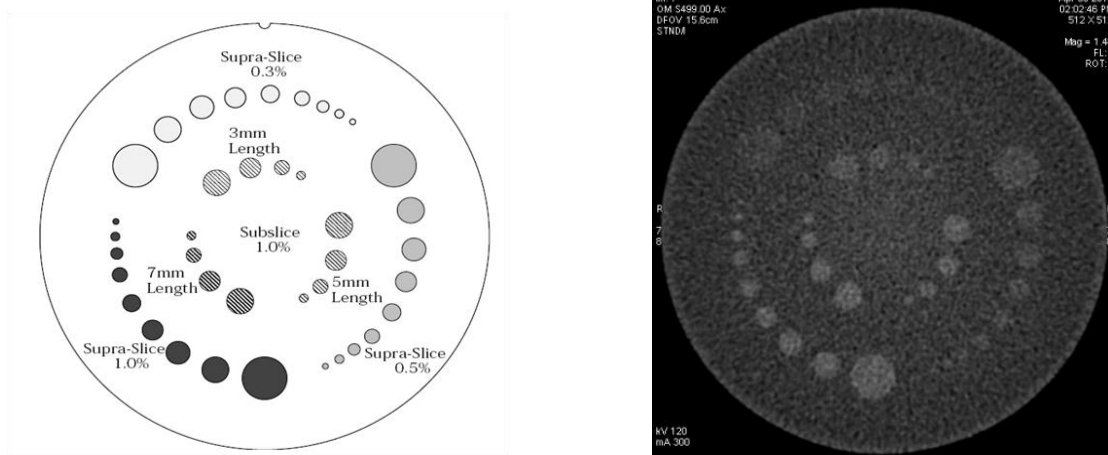**Technique:** 120 kVp, 300 mA, 1.0 sec, 250 mm FOV

Figure VII Low contrast detectability module

Results: Pass

Supra-slice	Nominal target contrast levels	Hole	%Contrast
	0.30%	5	1.8
	0.50%	8	1.5
	1%	9	2
Sub-slice	**Nominal target contrast levels**	**Hole**	**%Contrast**
	3 mm Length	4	3
	5 mm Length	4	5
	7 mm Length	4	7

14. Slice Thickness Accuracy

Purpose: To Determine the accuracy of the slice thickness.

Method: Set up as you would for beam profile measurement. Perform several scans with different programmed slice thicknesses under auto control. Scan the film with a densitometer and measure the full width at half maximum distance.

Technique: 120 kVp, 100 mA, 1.0 sec

Tolerance: should be < 1mm

Results: pass

Slice Thick in mm	Measured Thick in mm	Deviation
1.25	1.27	0.02
2.5	2.79	0.29
5	5.9	0.9

Deviation = | Indicated – Measured|

VITAE

Name: Miss Supawan Jivapong

Sex: Female

Nationality: Thai

Date of birth: August 10, 1980

Place of birth: Bangkok, Thailand

Home address: 51/27 Somruetai Village Moo 4 Thatalad, Sampran,

                        Nakornpathom, Thailand 73110

Qualification: Bachelor of Science (Radiological Technology)

                        Mahidol University, 2002

Job experience: Radiological technologist at Department of Radiology,

                        Faculty of Medicine, Siriraj Hospital for 10 years.